Zoosyst. Evol. 102 (1) 2026, 315–346 | DOI 10.3897/zse.102.183157

Redescription and systematics of *Oligodon ornatus* Van Denburgh, 1909, and two enigmatic related species (Squamata, Colubridae)

Yuhao Xu[1*], Tierui Zhang[2*], Benjamin W. Genter[3], Bo Cai[4], Shuo Qi[5], Shun Ma[4,6], Fanyue Sun[1], Chenxi Liao[7], Nikolay A. Poyarkov[8], Gernot Vogel[9], Justin L. Lee[10], Lifang Peng[1]

1 *State Key Laboratory of Plateau Ecology and Agriculture, Qinghai University, Xining 810016, Qinghai, China*
2 *The Anhui Provincial Key Laboratory of Biodiversity Conservation and Ecological Security in the Yangtze River Basin, College of Life Sciences, Anhui Normal University, Wuhu 241000, Anhui, China*
3 *Division of Herpetology, Florida Museum of Natural History, University of Florida, Gainesville, Florida 32611, USA*
4 *China-Croatia Belt and Road Joint Laboratory on Biodiversity and Ecosystem Services, Chengdu Institute of Biology, Chinese Academy of Sciences, Chengdu 610213, Sichuan, China*
5 *School of Ecology / School of Life Sciences, Sun Yat-sen University, Guangzhou 510275, Guangdong, China*
6 *University of Chinese Academy of Science, Beijing 100049, China*
7 *School of Materials Science and Engineering, Hainan University, Haikou 570228, Hainan, China*
8 *Department of Vertebrate Zoology, Lomonosov Moscow State University, Moscow 119234, Russia*
9 *Society for Southeast Asian Herpetology, D-69115 Heidelberg, Baden-Württemberg, Germany*
10 *Department of Ecology and Evolutionary Biology, University of Michigan, Ann Arbor, Michigan 48109, USA*

https://zoobank.org/FB57A0DD-AD33-47C9-86AF-DB8059A4AD8C

Corresponding authors: Lifang Peng (lifang@qhu.edu.cn); Justin L. Lee (justinllee@verizon.net)

Academic editor: Justin Bernstein ♦ **Received** 21 December 2025 ♦ **Accepted** 18 January 2026 ♦ **Published** 11 February 2026

Abstract

On the basis of molecular and morphological data, we re-evaluate the systematics of three closely related species of *Oligodon* Fitzinger, 1826 with unclear relationships: *Oligodon ornatus* Van Denburgh, 1909, *Oligodon lungshenensis* Zheng & Huang, 1978, and *Oligodon bivirgatus* Qian, Qi, Shi, Lu, Jenkins, Mo & Li, 2021. Recent phylogenetic studies recovered two divergent lineages of *O. ornatus* that render this species paraphyletic relative to *O. bivirgatus*. An examination of genetically identified material indicates that one of the two clades represents *O. ornatus*, while the other represents *O. lungshenensis*, thus resolving the paraphyly. Detailed descriptions of hemipenial morphology for all three species are provided, and all three species are redescribed and re-diagnosed, providing an updated framework for their identification. One male *O. bivirgatus* exhibits a color pattern differing from the type series, but this variation is likely intraspecific in nature as it does not correspond with sexual dimorphism. While mitochondrial DNA sequences revealed low to moderate pairwise genetic distances between species, haplotype networks from three nuclear loci recover limited evidence of allele sharing. We interpret these results as supporting the continued recognition of all three taxa as recently diverged yet distinct units at the species level. A unique temporal scale configuration observed in several *Oligodon* is discussed.

Key Words

China, molecular phylogeny, morphological characters, *Oligodon bivirgatus*, *Oligodon lungshenensis*, taxonomy, temporal scales

* These authors contributed equally to this work.

Copyright *Yuhao, X. et al.* This is an open access article distributed under the terms of the Creative Commons Attribution License (CC BY 4.0), which permits unrestricted use, distribution, and reproduction in any medium, provided the original author and source are credited.

Introduction

The kukri snake genus *Oligodon* Fitzinger, 1826, contains exceptional species diversity across the Asian continent (Fitzinger 1826; Jiang et al. 2025; Patel et al. 2025). Recent contributions based on molecular and morphological data have improved understanding of the phylogenetic relationships and evolutionary history within this genus (Jiang et al. 2025; Lee et al. 2025; Patel et al. 2025; Pauwels et al. 2025). Nonetheless, many *Oligodon* require re-evaluation using integrative taxonomic approaches. One of the eight major clades identified by a recent genus-wide phylogeny was the *Oligodon ornatus* Group, which comprises seven species, namely *O. catenatus* (Blyth, 1855), *O. bivirgatus* Qian, Qi, Shi, Lu, Jenkins, Mo & Li, 2021, *O. eberhardti* Pellegrin, 1910, *O. hamptoni* Boulenger, 1918, *O. lacroixi* Angel & Bourret, 1933, *O. lungshenensis* Zheng & Huang, 1978, and *O. ornatus* Van Denburgh, 1909 (Lee et al. 2024). These species are native to subtropical broadleaf, montane, and foothill forests of East and Southeast Asia (Zhao 2006; Orlov et al. 2010; Huang 2023). Among this group are three closely related taxa that constitute the primary focus in this study: *Oligodon bivirgatus*, *O. lungshenensis*, and *O. ornatus*.

Van Denburgh (1909) first described *Oligodon ornatus* based on a single specimen from "Shinchiku, Formosa" (= Hsinchu City, northern Taiwan Island, China) (Fig. 1). This was followed by two similar taxa: *Holarchus torquatus konishii* Oshima, 1910, also from north Taiwan Island, and *Simotes musyi* Roux, 1919 type locality from present-day Fujian Province, China. Steindachner (1914) synonymized the name *Holarchus torquatus konishii* under *O. ornatus* owing to geographic and morphological overlap, while Mell (1931) relegated *Simotes musyi* as a subspecies of *O. ornatus*. These changes led most authors to treat *O. ornatus* as monotypic, with Zhao et al. (1998) noting the characters separating the name *musyi* from nominotypical *ornatus* substantially overlap. *Oligodon lungshenensis* was described within Huang et al. (1978) from Longsheng County, Guangxi Zhuang Autonomous Region, China, and its taxonomic history has long been a subject of uncertainty. The primary source of this confusion was the description of *Oligodon guizhouensis* Li, 1979 from Yongle Town, Leishan County, Guizhou Province, China (~190 km W of Longsheng County), which was published a year after *O. lungshenensis* (Wu et al. 1979). Both taxa were morphologically similar to one another, yet only the latter (*O. guizhouensis*) was recognized after its description (Li 1989; Wu et al. 1985). The case

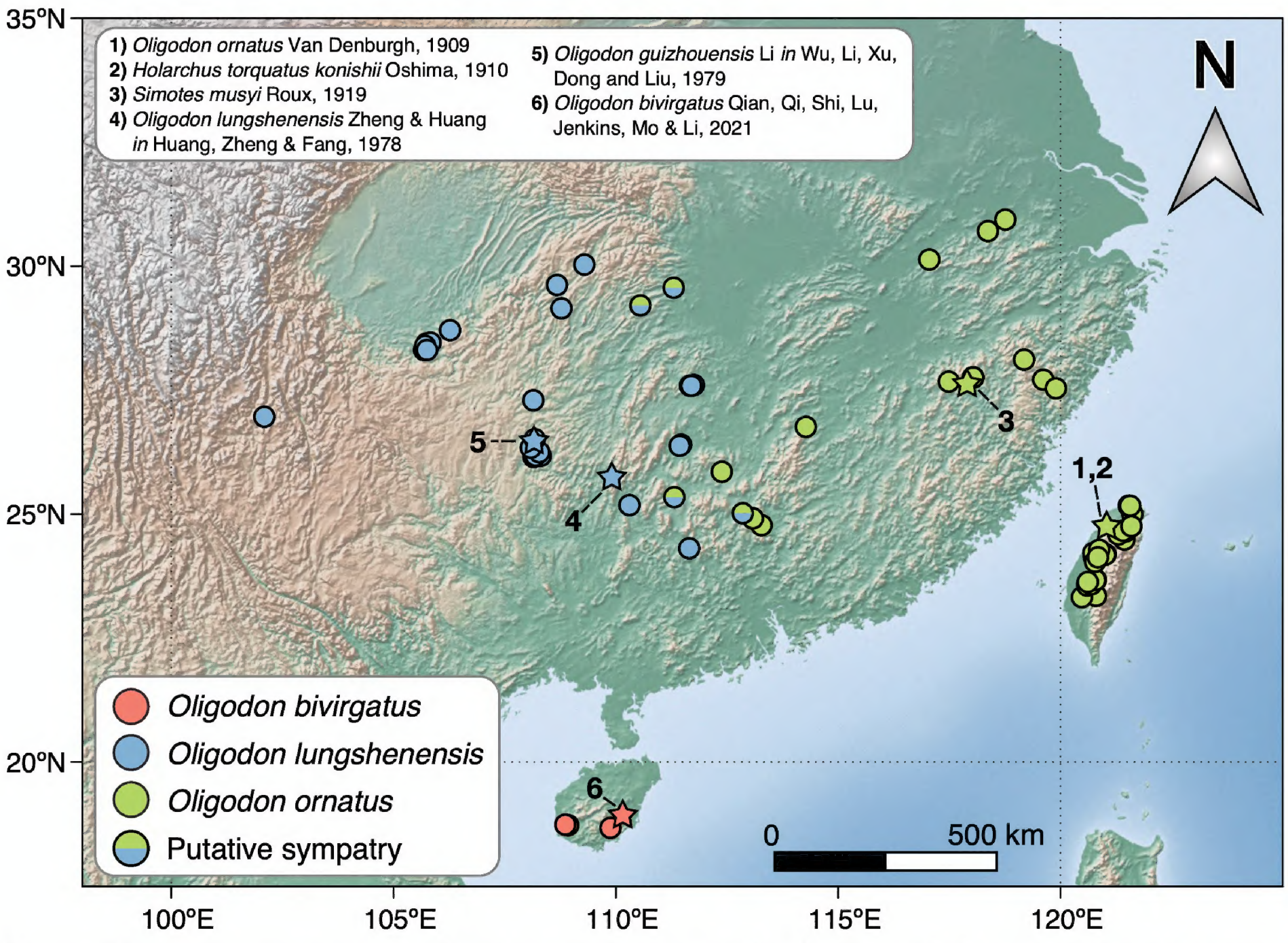

Figure 1. Map of eastern Asia showing the distribution of *O. bivirgatus*, *O. lungshenensis*, and *O. ornatus* based on voucher specimens, literature records, and electronic records (Suppl. material 1: table S1). Numbered stars represent type localities of species and junior synonyms.

was resolved when Zhao and Adler (1993) established that *Oligodon lungshenensis* and *O. guizhouensis* were conspecific and that the description of *O. lungshenensis* has precedence over *O. guizhouensis*. The most recent addition of the three species, *Oligodon bivirgatus*, was described based on two female specimens from Hainan Island, China (Qian et al. 2021). It noticeably differs from both *O. ornatus* and *O. lungshenensis* by possessing a two-striped dorsal coloration but is otherwise morphologically similar and exhibits a low genetic divergence based on mitochondrial DNA sequence data.

Several sampling issues have resulted in unclear phylogenetic relationships between all three focal species. Li et al. (2020) were the first authors to publish a multilocus phylogeny including *Oligodon ornatus*. Their tree topology divided *O. ornatus* into two divergent lineages, although this finding was not examined in detail. Qian et al. (2021) recovered *O. bivirgatus* as sister to *O. ornatus* based on 12s–16s ribosomal RNA sequences but only utilized samples of *O. ornatus* from southeast China and did not include sequences from the type locality. Wu et al. (2023) generated COI barcodes for *O. lungshenensis* and *O. ornatus* and recovered a sister relationship between each species, yet samples of *O. bivirgatus* were absent from their study. Lee et al. (2024) combined data from all three species and recovered a similar phylogenetic division of *O. ornatus* as Li et al. (2020). However, their trees placed *O. bivirgatus* between each *O. ornatus* lineage, rendering the latter species paraphyletic. These authors also refrained from sequencing COI barcode markers, so comparisons with samples of *O. lungshenensis* from Wu et al. (2023) could not be made. Consequently, Lee et al. (2024) referred to their two *O. ornatus* lineages as "*ornatus* clade 1" (including topotypic *O. ornatus*) and "*ornatus* clade 2" and recommended further taxonomic follow-up studies to resolve the issue. To that end, we use an expanded molecular and morphological dataset to test the validity of all three *Oligodon* species.

Materials and methods

Sampling

Newly reported specimens of *Oligodon* were collected/observed incidentally during herpetological field surveys across China. Voucher specimens were deposited in the herpetological collections of Anhui Normal University, Wuhu, Anhui, China (ANU), the Chengdu Institute of Biology, Chinese Academy of Sciences, Chengdu, Sichuan, China (CIB), and Qinghai University, Xining, Qinghai, China (QHU) after euthanasia with a buffered MS-222 (tricaine methanesulfonate) solution. All specimens were fixed in 10% formalin before being transferred to 70–75% ethanol. Tissue samples were removed from the liver before preservation and stored separately in 95% ethanol at –20 °C. To make further morphological comparisons, we studied previously deposited specimens in museum collections that were available to us and gathered existing morphological data associated with all three *Oligodon* species from the primary literature.

Molecular data

Tissue samples were sequenced for three mitochondrial genes (12s16s ribosomal RNA [12s16s], cytochrome oxidase I [COI], and cytochrome b [CytB]) and three nuclear genes (recombination activation gene 1 [Rag1], brain-derived neurotrophic factor [BDNF], and oocyte maturation factor Mos [c-mos]). Genomic DNA was extracted from each sample using a QIAamp DNA Mini Kit (QIAGEN, Changsheng Biotechnology Co. Ltd., Changchun, China). Polymerase Chain Reactions (PCRs) were performed using primers and amplification protocols described by Lee et al. (2024), except for COI, where the barcode primers Chmf4 and Chmr4 (Che et al. 2012) were used (Suppl. material 1: table S2). PCR products were sequenced externally by Shanghai Map Biotech Co., Ltd. (Shanghai, China). We used Geneious Prime (Biomatters Ltd.) to assemble and edit the sequence files and aligned them with existing DNA sequences using MAFFT version 7.0 (Katoh and Standley 2013). DNA sequences were added to a pruned molecular dataset containing existing genetic material from members of the *Oligodon ornatus* Group (Lee et al. 2024) and additional samples from GenBank (Suppl. material 1: table S3). We ran two independent phylogenetic analyses on different molecular datasets. The first dataset was a concatenated alignment consisting of two mitochondrial genes (12s16s and CytB) and all three nuclear genes. Three additional species of *Oligodon* were added as outgroups due to their phylogenetic position at the base of the genus: *Oligodon calamarius* (Linnaeus, 1758), *Oligodon signatus* (Günther, 1864), and *Oligodon transcaspicus* (Nikolsky, 1902). The final concatenated alignment was 5,106 base pairs (bp) long with 714 distinct patterns and 394 parsimony-informative sites; individual gene lengths were 1,904 bp (12s–16s), 1,103 bp (CytB), 867 bp (Rag1), 686 bp (BDNF), and 564 bp (c-mos). A separate phylogenetic analysis without outgroup taxa was performed on an alignment containing COI sequences only. This was done to include additional DNA barcode samples from GenBank, which lacked any additional mitochondrial or nuclear data associated with them (Suppl. material 1: table S3). The COI gene alignment was 658 bp long with 96 distinct patterns and 64 parsimony-informative sites.

After inspecting sequences to ensure translation, we used the command-line implementation of IQ-TREE version 2.1.2 to generate a maximum likelihood (ML) phylogeny and used BEAST2 version 2.7.6 to generate a Bayesian Inference (BI) phylogeny (Bouckaert et al. 2014; Minh et al. 2020). Only an ML tree was generated for the COI barcode dataset. For the ML tree, we used ModelFinder in IQ-TREE to select the best substitution model for each gene and codon position (Kalyaanamoor-

thy et al. 2017). The TIM2+F+G4 model was selected for the first+second and third mtDNA (12s16s + CytB) codon positions; the HKY+F+I model was selected for all remaining codon positions (Rag1, BDNF, and c-mos). The ML consensus tree was generated after 1000 ultrafast bootstrap replicates (UF BS) and 1000 Shimodaira–Hasegawa approximate likelihood-ratio tests (SH-aLRT). The BI tree was generated in BEAST2 under a Yule Model with default parameters. We used BModelTest to estimate the best-scoring substitution model for each partition. Three separate runs in BEAST2 were conducted, each with a Markov-Chain Monte Carlo (MCMC) chain of 50 million generations and a sampling rate of 5000. The three runs were combined in LogCombiner after dropping the first 10% as burn-in. We used Tracer 1.7.1 (Rambaut et al. 2018) to check that the combined chains reached convergence and that effective sample sizes of posterior and likelihood values were above 200. A final ultrametric maximum clade credibility tree was built using TreeAnnotator version 2.7.4. (Bouckaert et al. 2014). Nodes with SH-aLRT tests > 80.0%, UF BS values > 95%, and Bayesian posterior probabilities (BI PP) > 0.95 were considered strongly supported; lower values were considered poorly supported. Pairwise genetic distances (p-distances) were calculated using the dna.dist() function in the R-package ape version 5.8 (Paradis and Schliep 2019) under a raw model with pairwise deletion set to "TRUE."

We examined variation in nuclear DNA sequences by generating haplotype visualization networks in Hapsolutely (Vences et al. 2024), a program part of the iTaxoTools interface (Vences et al. 2021). Missing data in each nuclear dataset were removed prior to generating haplotype networks, resulting in alignments consisting of 867 bp (Rag1), 674 bp (BDNF), and 511 bp (c-mos). Heterozygous sites were coded according to their corresponding IUPAC nucleotide codes. All gene alignments were phased prior to visualization using the PHASE setting in Hapsolutely (Stephens et al. 2001). Phase (-p) and allele (-q) certainty thresholds were each set to 0.75, while iteration and burn-in values were set to 1000. Resulting haplotype networks were generated under the TCS algorithm. We note our sample size was highest for the Rag1 locus ($N = 11$), while haplotype networks of BDNF and c-mos were based on a lower number of sequences ($N = 10$).

Morphological data

We examined preserved specimens of *Oligodon bivirgatus*, *O. lungshenensis*, and *O. ornatus* for morphological comparisons, including the holotype of *Simotes musyi*. Data on the type series of *O. ornatus*, *O. bivirgatus*, *O. lungshenensis* (including its synonym *O. guizhouensis*), and one of the junior synonyms of *O. ornatus* (*Holarchus torquatus konishii*) come from original descriptions (Van Denburgh 1909; Oshima 1910; Huang et al. 1978; Wu et al. 1979; Qian et al. 2021). Data on other referred specimens come from the primary literature (Zhao et al. 1986; Gong and He 2008; Yuan et al. 2010; Luo et al. 2010; Ran et al. 2012; Dong et al. 2023; and Liu et al. 2025). Body and tail lengths were measured to the nearest millimeter by straightening specimens along a flexible ruler. Head dimensions were measured with digital calipers to the nearest 0.1 mm. Methodology for counting ventral scales follows Dowling (1951). The tail tip was not included in the number of subcaudals. Head scale counts are given in left/right order. We use the term "temporolabial" interchangeably to describe the enlarged lower anterior temporal scale in select members of *Oligodon* that is wedged between the two posteriormost supralabials and blocked from contacting the postocular and lip (McDowell 1967; see Discussion for further explanation on this matter). Maxillary tooth sockets were counted by reflecting soft tissue with forceps or dissecting pins to reveal the upper jaw. Terminology used to describe head scale sutures and their angles follows Kaiser et al. (2019). Symmetric characters are given in left/right order. The sex of preserved specimens was determined by making a small ventral incision at the underside of the tail to check for the presence or absence of hemipenes, whereas the sex of uncollected individuals was determined by gently pressing the base of the tail to observe whether the hemipenes were everted. When present, hemipenes were everted on the left side of fresh or preserved male specimens. Everted hemipenes were prepared using colored petroleum jelly following protocols adapted from Myers and Cadle (2003) and Jiang (2010). Terminology for hemipenial characters follows Dowling and Savage (1960), Zhang et al. (1984), and Ren et al. (2022, 2025a). Hemipenial images were captured using a digital camera. Dorsal bands were only counted on the left side of the body and tail. Nuchal markings, or secondary markings in between, were not included in the final count. Bands covering the cloacal plate were included in the body band count. Bands covering the tip of the tail were included in the tail band count.

Linear measurements and meristic characters abbreviated in-text generally follow Darko et al. (2022), but some are modified so they are consistent with earlier descriptions of *Oligodon* in the literature: snout vent length (**SVL**); tail length (**TailL**); total length (**TotalL**); tail length / total length ratio (**TailLR**); head length, measured from retroarticular process of the mandible to snout tip (**HeadL**); head width, measured at the widest point of the head (**HeadW**); snout length, measured from anterior margin of the eye to snout tip (**SnoutL**); eye diameter, measured as the longest horizontal distance across the eye (**EyeD**); frontal scale length (**FrontalL**); frontal scale width (**FrontalW**); interorbital distance, measured from lateral ends of each supraocular between the eyes (**IOD**); internarial distance, measured between midpoints of each nostril (**IND**). Meristic characters examined include maxillary teeth (**MT**); dorsal scale rows (**DSR**); ventral scales (**VEN**); subcaudal scales (**SC**); total body scales, the number of ventral, subcaudal scales plus an additional count of one to include the cloacal plate (**TOTAL**);

subcaudal ratio, the ratio between the number of subcaudals and total body scales (**SCR**); condition of internasal scales (**INS**); supralabials (**SL**); number of supralabials in contact with the eye (**SLE**); infralabials (**IL**); preocular scales (**PreOc**); postocular scales (**PostOc**); and temporal scale formula (**TEMP**). Color pattern abbreviations include body bands (**BBand**), tail bands (**TBand**), and total bands (**TotBand**).

Statistical analyses

We examined whether *O. bivirgatus*, *O. lungshenensis*, and *O. ornatus* were morphologically differentiated from one another. Univariate analyses were conducted on males ($N = 28$), females ($N = 18$), and both sexes ($N = 46$) (Raw data presented in Suppl. material 1: tables S4, S5). We also tested the presence of sexual dimorphism in three body scale characters (VEN, SC, TOTAL) and two ratios (TailLR and SCR) using Student's t-tests. Nine characters (TailLR, VEN, SC, TOTAL, SCR, SL, SLE, IL, ILCS) were used in the univariate analysis. Shapiro–Wilk Tests and Levene's Tests were first used to test that each character followed normal distributions and had equal variance. We then conducted a one-way analysis of variance (ANOVA) followed by a Tukey's Honestly Significant Difference (HSD) post-hoc test to determine whether morphological characters were significantly different between species. A principal components analysis (PCA) was performed using the *prcomp*() function in R to investigate whether visible structure in morphological variation exists. Only seven meristic characters (VEN, SC, TOTAL, SCR, SL, IL, ILCS) were used in the PCA, and the analysis was only performed on a subset of male specimens ($N = 17$) due to unequal sample sizes and missing data. Data used in the PCA were log-transformed to reduce the influence of outliers. We considered statistically significant differences to have p-values less than 0.05. All statistics were conducted in R version 4.5.0 R Core Team.

Museum acronyms and abbreviations

Museum and other natural history collection acronyms are provided as follows: **AMNH**: American Museum of Natural History, New York, USA; **ANU:** Anhui Normal University Museum, Wuhu, China; **CAS:** California Academy of Sciences, San Francisco, USA; **CIB/CIB-CAS**: Museum of Herpetology, Chengdu Institute of Biology, Chinese Academy of Sciences, Chengdu, China; **CTS**: Zoological Museum of Chongqing Tsinghua High School, Chongqing, China; **CWNU**: China West Normal University, Nanchong, China; **FMNH**: The Field Museum, Chicago, USA; **HNNU**: Hunan Normal University, Changsha, China; **FNU**: Fujian Normal University, Fuzhou, China; **KIZ**: Kunming Institute of Zoology, Chinese Academy of Sciences, Kunming, China; **NHMB**: Natural History Museum Basel, Basel, Switzerland; **NHMG**: Natural History Museum of Guangxi Zhuang Autonomous Region, Nanning, China; **NTUM**: National Taiwan University Museum, Taipei, China; **QHU**: Qinghai University, Xining, China; **SYNU**: Shenyang Normal University, Shenyang, China; **SYS**: Museum of Biology, Sun Yat-sen University, Guangzhou, China; **TRU**: Tongren University, Tongren, China; **UMMZ**: Museum of Zoology, University of Michigan, Ann Arbor, USA; **USNM**: National Museum of Natural History, Smithsonian Institution, Washington, USA; **XDSNR**: Hubei Xingdoushan National Nature Reserve, Enshi, China; **YBU**: Yibin University, Yibin, China; **ZMU**: Zunyi Medical University, Zunyi, China; **ZMMU**: Zoological Museum of Lomonosov Moscow State University, Moscow, Russia. Other abbreviations used in-text are listed as follows: **Is**: Island; **Mt.**: Mountain; **Mts.**: Mountains; **NP**: National Park; **NR**: Nature Reserve; **WS**: Wildlife Sanctuary; **asl.**: above sea level.

Assessment of threat status

Only two of the three *Oligodon* in this study (*O. ornatus* and *O. lungshenensis*) have conservation assessments published by the IUCN Red List (Zhou et al. 2012; Rao et al. 2024), and some of the records used in these reports are based on specimens that may represent misidentifications (Zhao 2002, 2006). To circumvent these issues, we generated updated conservation status assessments of each species, following the categories and criteria adopted by the IUCN Red List (https://www.iucnredlist.org/resources/redlistguidelines). This framework classifies species according to their extinction risk and provides a clear and objective system that is widely applicable and has been extensively validated (Maes et al. 2015). Among the five criteria defined by the IUCN, which include Criterion A (population reduction), B (geographic range), C (small population size and decline), D (very small or restricted population), and E (quantitative analysis of extinction risk) (IUCN 2012), reliable population data were not available. Therefore, we assessed extinction risk using Criteria B and D. Geographic range metrics, including the extent of occurrence (EOO) and the area of occupancy (AOO), were calculated using the online tool GeoCAT (https://geocat.iucnredlist.org; last accessed 15 January 2026).

Results

Molecular results

Phylogenetic relationships in the *O. ornatus* group were congruent across concatenated ML and BI tree topologies, and no conflicting tree topologies were noted (Fig. 2). Like earlier studies (Lee et al. 2024), *O. ornatus* sensu lato comprised two genetically divergent clades. *O. ornatus* "clade 1" was recovered as sister to a clade containing *O. bivirgatus* and *O. ornatus* "clade 2"

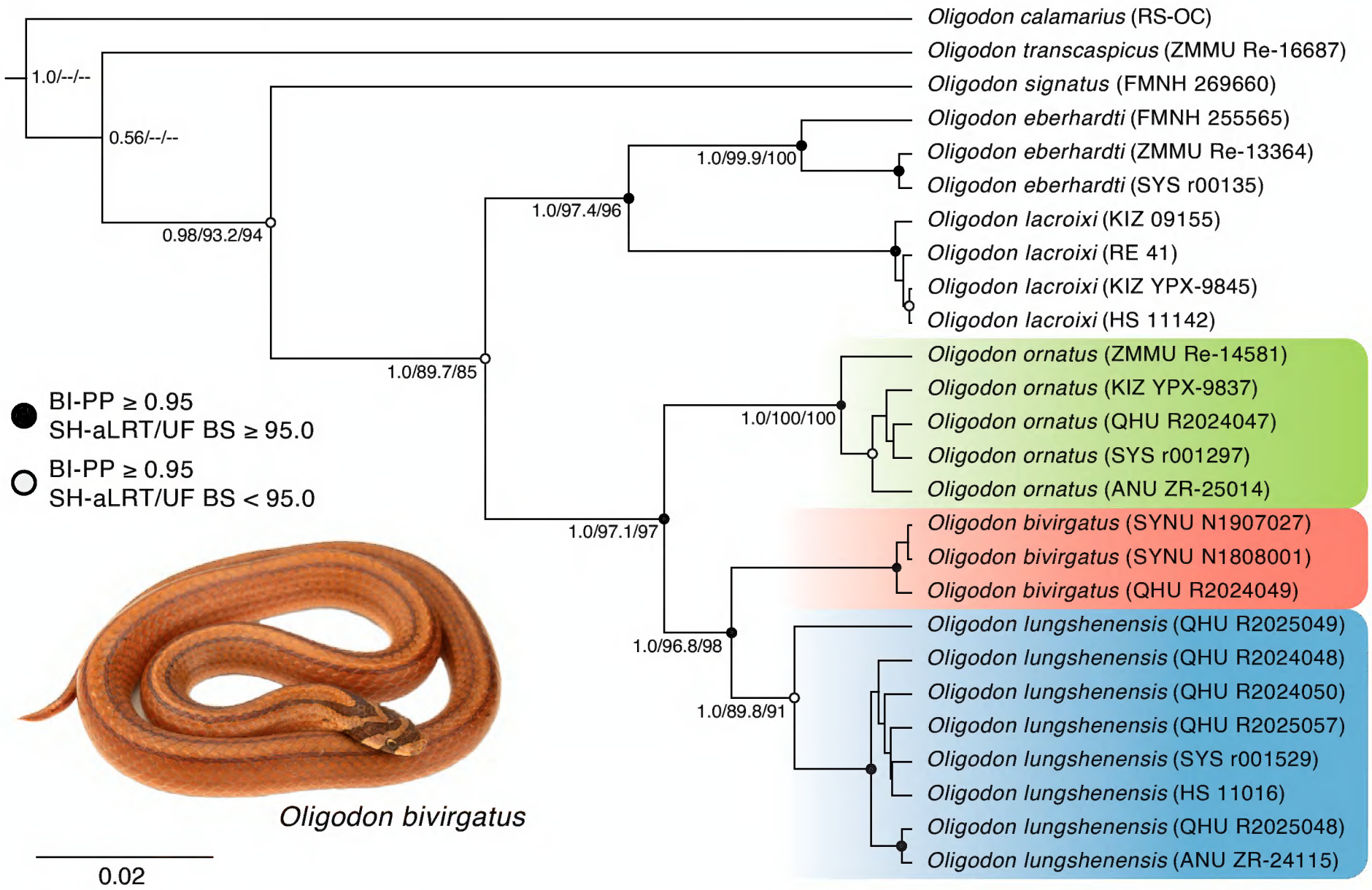

Figure 2. Bayesian phylogeny of the *Oligodon ornatus* group based on concatenated mitochondrial and nuclear DNA sequence alignments. Both ingroup and outgroup taxa are shown. Numbers at nodes correspond to BI PP / SH-aLRT / UFBS values. Photograph of *Oligodon bivirgatus* (iNaturalist 298113949) by Benjamin W. Genter.

(= *O. lungshenensis*) with strong support (BI PP = 1.0 / SH-aLRT = 97.1 / UF BS = 97). All three focal lineages were strongly supported in each analysis, although the node comprising *O. lungshenensis* received lower support in the ML tree (1.0/89.8/91). Relationships in the ML COI barcode phylogeny were congruent with concatenated ML+BI trees, albeit with poorer support at several deeper internal nodes (Suppl. material 1: fig. S1). Topotypic samples of *O. ornatus* from Taiwan, China, were recovered in *O. ornatus* clade 1, and all morphologically examined specimens in that clade possessed internasal and prefrontal scales, a diagnostic character separating *O. ornatus* from *O. lungshenensis*. Likewise, newly sequenced samples identified as *O. lungshenensis* were recovered in *O. ornatus* clade 2, including one specimen (QHU R2024050) collected ~65 km southeast of the type locality (Longsheng County, Guangxi Zhuang AR, China). These specimens, plus the vouchered material sampled in Lee et al. (2024), have fused internasals, agreeing with *O. lungshenensis*.

Genetic distances between focal species were low to moderate (Table 1). For 12s16s, *Oligodon lungshenensis* was separated from *O. ornatus* by p-distances of 1.97%–3.41% ($\bar{x}$ = 2.82%) and from *O. bivirgatus* by only 1.63%–2.36% ($\bar{x}$ = 2.02%). These species comparisons were higher when COI and CytB p-distances were compared; mean sequence divergences between *O. lungshenensis* versus *O. ornatus* ranged from 4.50–5.66%, and divergences between *O. bivirgatus* versus *O. lungshenensis* were 3.1–3.12% (both mean values for COI and CytB, respectively; Table 1). Sequence divergences between *O. bivirgatus* and *O. ornatus* were 2.38–4.02% ($\bar{x}$ = 3.32%) for 12s16s, 4.72%–5.93% ($\bar{x}$ = 5.39%) for COI, and 5.41–5.81% ($\bar{x}$ = 5.61%) for CytB. Notably, intraspecific p-distances were high in *O. lungshenensis* (12s16s: 0.00%–1.55%, COI: 0.00%–2.18%, CytB:

Table 1. Uncorrected pairwise distances (p-distances; given as percent values) within and between *O. bivirgatus*, *O. lungshenensis*, and *O. ornatus*, based on mitochondrial *12S–16S*, *COI*, and *CytB* gene sequences. Mean values are given in parentheses.

Species Pair	12S–16S	COI	CytB
bivirgatus–bivirgatus	0.00%–0.11% (0.05%)	0.00%	0.00%
bivirgatus–lungshenensis	1.63%–2.36% (2.02%)	2.90%–3.52% (3.1%)	2.91%–3.73% (3.12%)
bivirgatus–ornatus	2.08%–3.29% (2.87%)	4.72%–5.93% (5.39%)	5.59%–6.32% (5.96%)
lungshenensis–lungshenensis	0.00%–1.55% (0.49%)	0.00%–2.18% (0.51%)	0.00%–3.08% (0.87%)
lungshenensis–ornatus	1.97%–3.41% (2.82%)	3.81%–5.82% (4.5%)	5.13%–6.32% (5.66%)
ornatus–ornatus	0.00%–0.95% (0.34%)	0.00%–2.74% (1.33%)	0.00%–3.42% (1.75%)

0.00%–3.08%) and in some cases approached the interspecific p-distances recorded between *O. bivirgatus* and congeners (Table 1). Phased nuclear DNA haplotype networks showed differing patterns of genetic differentiation between *O. bivirgatus*, *O. lungshenensis*, and *O. ornatus* (Fig. 3). In Rag1, there were no alleles shared between *O. ornatus* and *O. lungshenensis*, and both species were separated by at least one mutational step. However, *O. bivirgatus* and two samples of *O. lungshenensis* grouped together into a single Rag1 allele (Fig. 3). No evidence of allele sharing was detected between *O. bivirgatus* and *O. lungshenensis* in the c-mos and BDNF datasets, and each species was separated by at least two mutational steps. Two phased BDNF haplotypes (QHU R202048, QHU R2025057) and one phased c-mos haplotype (QHU R2025057) of *O. lungshenensis* grouped together with three samples of *O. ornatus*.

Morphological results

Morphological data used in the statistical analyses are presented in Suppl. material 1: table S5. Results from the ANOVA and Tukey's HSD post-hoc tests revealed only five characters that exhibited significant differences between male populations of the three *Oligodon* species (Table 2). No statistical differences were detected between females, and only four characters were significant-

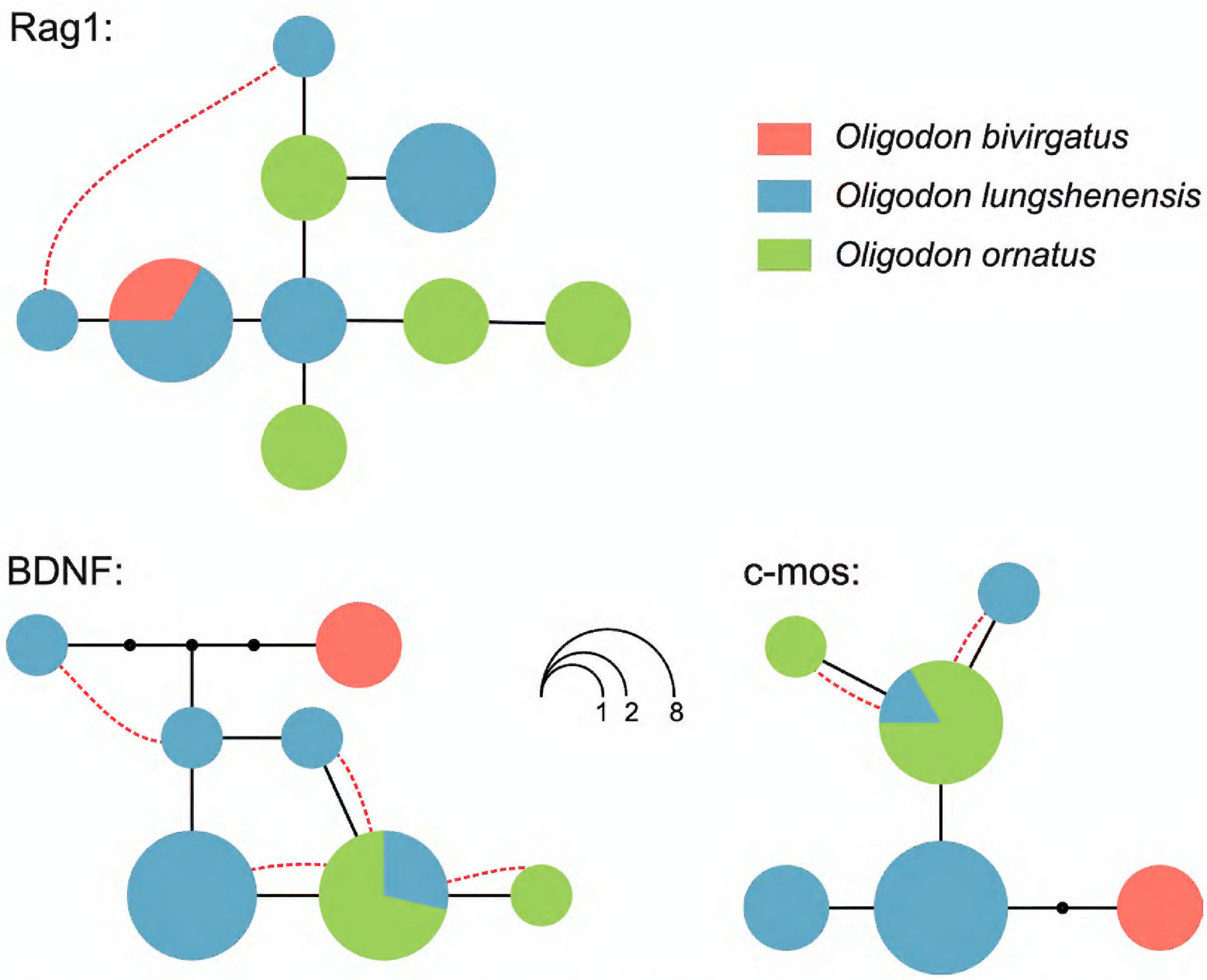

Figure 3. Haplotype networks of phased nuclear gene alignments for *Rag1* (11 specimens), *BDNF* (10 specimens), and *c-mos* (10 specimens). Each specimen is represented by two sequences. Red lines indicate co-occurrence of different alleles within the same individual.

Table 2. Pairwise comparisons among three species of *Oligodon*, based on ANOVA and Tukey's HSD post hoc tests for males and for combined sexes (the ANOVA revealed no differences in the female-only sample). Characters with significantly different p-values are highlighted in bold. Morphological character acronyms are provided in the Materials and methods.

Species Pair (Males)	***lungshenensis–bivirgatus***	***ornatus–bivirgatus***	***ornatus–lungshenensis***
TailLR	0.0265384	0.9999813	**0.001585**
VEN	**0.0000584**	**0.0015058**	0.1997676
SC	0.950215	0.2247209	**0.0109507**
TOTAL	**0.0003524**	**0.0006256**	0.9993503
SCR	0.0759088	0.8971941	**0.0011733**
Species Pair (Both Sexes)	***lungshenensis–bivirgatus***	***ornatus–bivirgatus***	***ornatus–lungshenensis***
TailLR	0.0504859	0.8055912	**0.0005072**
SC	0.4074204	0.3036361	**0.000495**
SCR	0.0510188	0.808402	**0.0003475**
IL	0.3982677	0.0657011	0.2437826

ly different when females/males were combined (Table 2). These results indicate male *O. bivirgatus* have a lower ventral and total body scale count than male *O. lungshenensis* and *O. ornatus*. Additionally, *O. lungshenensis* has a lower mean relative tail length (TailLR), subcaudal ratio, and subcaudal scale values than *O. ornatus* (these characters were significantly different in both males and when sexes were combined; Table 2). The PCA recovered males of all three species in separate positions along the ordination of the first two principal components, which accounted for 64.8% of the total variance (Fig. 4; Table 2, Suppl. material 1: table S6); though, there was slight overlap between *O. lungshenensis* and *O. ornatus*. Subcaudal scales and the subcaudal ratio contributed the highest to PC1 (42.3% of variance). Ventral scales, total body scales, and infralabials contributed the highest to PC2 (25.2% of variance).

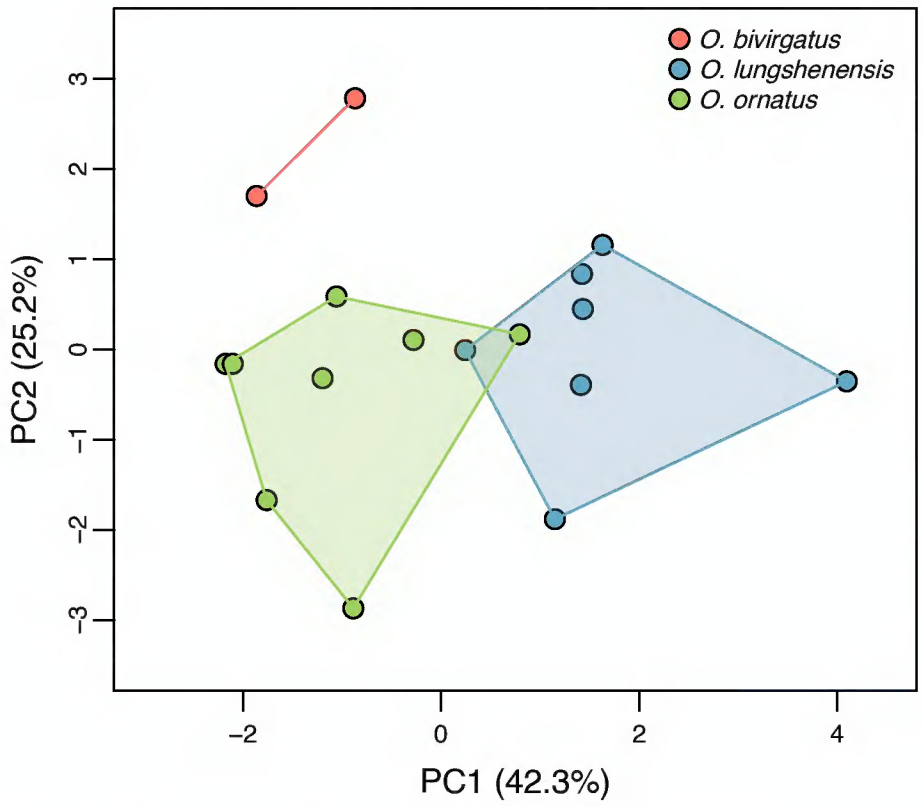

Figure 4. Principal components analysis (PCA) based on seven morphological characters showing separation among males of *Oligodon bivirgatus*, *O. lungshenensis*, and *O. ornatus*.

Taxonomic conclusion

Both lines of evidence resolve the non-monophyly of *Oligodon ornatus* reported by Lee et al. (2024). Each of the genetically divergent clades from earlier studies can now be matched to both *O. ornatus* and *O. lungshenensis*, respectively. Mitochondrial sequence divergences between *O. bivirgatus* and *O. lungshenensis* were low compared to p-distance ranges reported in other *Oligodon* sister species pairs (Table 1) (Lee et al. 2024). However, both species are morphologically differentiated from one another based on color pattern, scalational characters, and differences in hemipenial ornamentation. Moreover, *O. bivirgatus* and *O. lungshenensis* were consistently separated by multiple mutational steps based on nuclear haplotype analyses (Fig. 3), exhibit allopatric distributions, and do not overlap in distributions, supporting their status as evolutionarily independent lineages (De Queiroz 2007). These congruent results indicate all three focal taxa ought to remain valid at species rank, and accordingly, we redescribe them below with expanded morphological data, including the first hemipenial descriptions of *O. bivirgatus* and *O. lungshenensis*.

Taxonomic accounts

Oligodon ornatus Van Denburgh, 1909

Figs 5–8, Suppl. material 1: table S4

Ornate Kukri Snake / 饰纹小头蛇 (Pinyin: Shì Wén Xiǎo Tóu Shé)

Synonymy. *Holarchus torquatus konishii* – Oshima (1910): 196–197.

Simotes musyi – Roux (1919): 62–63.

Holarchus ornatus musyi – Mell (1931): 211.

Type material. *Holotype.* • CAS 18005 (adult male), collected on 7 March 1909 by V. Kühne [J.C. Thompson]. Type locality: "Shinchiku, Formosa" [= Hsinchu City, Taiwan Province, China].

Specimens examined (*N* = 11). China. Anhui Province. • QHU R2024047 (Field NO. LFR 2024097; adult male), a road killed specimen from Xuanzhou District, Xuancheng Prefecture (30.7063°N, 118.7915°E; 209 m asl.) collected by Y.H. Xu. **Fujian Province.** • CIB 9968 (juvenile), • CIB 9969 and • CIB 78058 (two adult males), • CIB 9970 (adult female), and • ANU ZR25014 (adult male), all from Wuyishan (formerly "Ch'ungan Hsien"), Nanping Prefecture (approx. 27.756°N, 118.035°E), no other collection data available; • NHMB unnumbered (adult male), holotype of *Simotes musyi*, from Wuyishan (formerly "Ch'ungan Hsien"), Nanping Prefecture (approx. 27.756°N, 118.035°E) donated by M. Musy, date unknown. **Jiangxi Province.** • SYS r001297 (adult male) from Jinggangshan National Nature Reserve, Jinggangshan City, Ji'an Prefecture (approx. 26.759°N, 114.274°E), collected on 30 July 2015 by the team of Yingyong Wang. **Hunan Province.** • CIB-CAS 102876 (adult male), from Yizhang County, Chenzhou City (approx. 24.966°N, 112.851°E). **Taiwan Province.** • UMMZ 182640 (adult male) from "Nan-Tou, Chi-Tou" [=Xitou Nature Education Area, Nantou County] (approx. 23.674778°N, 120.796833°E) collected 20 May 1983; • ZMMU Re-14581, from Beiheng Road, Mingchi Forest Area, Fuxing District (approx. 24.644°N, 121.462°E).

Other reported specimens (*N* = 15). China. Fujian Province. • FMNH 24963, • FMNH 24964, • FMNH 24965, • AMNH R-33756, • AMNH R-33757, • AMNH R-33592, • AMNH R-33593, • AMNH R-33594, • AMNH R-33595, all from Guadun Village, Wuyishan NP, Nanping Prefecture (formerly "Kuatun Village") (27.735229°N, 117.641156°E), no other data available, reported by Pope (1929) and Pope (1935). **Guangdong Province.** • KIZ YPX23180 from Nanling National Forest Park (approx. 24.913°N, 113.083°E) and KIZ YPX9837 from Ruyuan Yao Autonomous County, Shaoguan City (approx. 24.913°N, 113.082°E); no other data available, reported by Wu et al. (2023); unnumbered specimen also

from Nanling National Forest Park (approx. 24.913°N, 113.083°E); no other data available, reported by Gong and He (2008). **Hunan Province.** • HNNU 59-14 (adult female), from Jiangyong County, Yongzhou City (approx. 25.274°N, 115.344°E); • HNNU 59-46 (adult female), from Cili County, Zhangjiajie City (approx. 29.431°N, 111.139°E); and • HNNU 810705 (adult female), from Zhangjiajie City (approx. 29.120°N, 110.485°E), no other data available, reported by Shen et al. (2014). **Taiwan Province.** • NTUM 84, the holotype of *Holarchus torquatus konishii*, from New Taipei City, Shenkeng (approx. 25.003°N, 121.617°E), no other data available, reported by Oshima (1910). Literature data from reported specimens are mentioned in the description. For electronic records, refer to Suppl. material 1.

Revised diagnosis. A medium-sized *Oligodon*, tail moderately long (TailLR 0.119–0.163; in males 0.145–0.163; in females 0.119–0.128). Dorsal scales in 15–15–15 rows, all smooth, no reductions. Ventral scales 160–185, no dimorphism (160–173 in males and 171–185 in females), no keeling. Cloacal plate divided. Subcaudals 31–43 (34–43 in males, 31–35 in females), paired. Total body scales 199–221 (199–217 in males, 203–221 in females). Subcaudal ratio 0.153–0.205, no (in males 0.171–0.205, in females 0.153–0.158). Maxillary teeth 7–8, posterior three teeth slightly enlarged and blade-like. Internasals present. Loreal absent, preocular 1, presubocular absent, postoculars 2, temporals 2+2 (rarely 2+1, 1+2, or 1+1). Temporolabial scale present (rarely fused). Supralabials 6 (rarely 5), 3rd–4th in contact with the eye (rarely 2nd–3rd in contact). Infralabials 6 (rarely 7), first 1–4 in contact with anterior chin shields. Dorsal surface light brown or grayish brown with a broad brown paravertebral stripe and a narrower lateral stripe on either side of body, both extending from nape to tail. Middorsal line between paravertebral stripes, same color as remaining body. A total of 10–12 irregular dorsal bands present (8–10 on body, and 1–3 on tail), some specimens exhibiting secondary bands or spots concentrated along the middorsal or paravertebral regions. Median portions of each band brown, edges normally dark brown or black. Head markings include ocular bar, temporal bar, and nuchal chevron. Ventral surface white with lateral series of black alternating rectangular blotches on ventral scales and a broad red midventral stripe in life. Hemipenis unilobed, simple sulcus spermaticus, spines uniformly sized, absent on basal one-eighth of organ and parts of apical surface.

Description and variation. *Oligodon ornatus* was previously considered to be widely distributed across numerous provinces in eastern China, including Anhui, Fujian, Guangxi, Guangdong, Hainan, Hunan, Jiangxi, Sichuan, Zhejiang, and Taiwan Island (Van Denburgh 1909; Pope 1935; Chen 1991; Zhao et al. 1998; Kadoorie Farm and Botanic Garden 2001; Zhao 2006; Gong and He 2008; Shen et al. 2014). However, many of these records represent misidentifications, especially those from Guangxi, Sichuan, Hainan, and parts of Hunan. Although specimens reported by Pope (1935) and Zhao et al. (1998) were all collected from Fujian Province, neither study provided detailed morphological data for each specimen, making detailed comparisons impossible. Furthermore, Zhao (2006) offered a general description of the species, but many records included in that study are likely inaccurate. Therefore, the redescription of *O. ornatus* in the present study is based only on examined material ($N = 11$), the original description (Van Denburgh 1909) ($N = 1$), and literature that includes specific specimen information and diagnostic characters (Gong and He 2008) ($N = 1$). The main morphological characters of the specimens used in this study are listed in Suppl. material 1: table S4.

Body slender, subcylindrical. Head oblong, slightly distinct from neck. Snout elongate, narrowing in width in dorsal profile, slightly truncate in lateral profile. Eyes moderate relative to head, pupil round. Nostrils small, subelliptical, pointed laterally. Tail moderate, tapering gradually to sharp pointed tip. Adult SVL 292–559 mm, TailL 51–95 mm, TotalL 343–654 mm ($N = 10$). One immature specimen (CIB 9968) measured 147 mm SVL, 25 mm TailL (TotalL 172 mm). The largest specimen an adult male (CIB 78058) measuring 559 mm SVL and 95 mm TailL. Largest female (uncataloged specimen fide. Gong and He (2008) measured 458 mm SVL, 67 mm TailL. Head measurements ($N = 8$ unless noted otherwise): HeadL 9.2–18.4 mm, HeadW 5.8–13.6 mm, SnoutL 2.9–5.6 mm, EyeD 1.5–3.0 mm, FrontalL 2.8–6.1 mm, FrontalW 2.3–5.2 mm, IOD 3.2–7.8 mm, IND 3.0–5.3 mm. TailLR 0.119–0.163 (0.145 ± 0.013; $N = 10$), in males 0.145–0.163 ($\bar{x} = 0.151 \pm 0.007$; $N = 8$), in females 0.119–0.128 ($\bar{x} = 0.123 \pm 0.006$; $N = 2$). Slight sexual dimorphism present (Student's t-test $P = 0.04887$). Head measurement ratios (all $N = 8$): HeadW/HeadL 0.52–0.74, SnoutL/HeadL 0.26–0.35, EyeD/SnoutL 0.43–0.57, EyeD/HeadL 0.13–0.17, FrontalL/FrontalW 1.09–1.33.

Body scalation. Dorsal scales in 15–15–15 rows, all smooth with no reductions. Ventral scales 160–185 ($\bar{x} = 168.5 \pm 7.1$; $N = 12$), in males 160–173 ($\bar{x} = 166.6 \pm 5.1$; $N = 10$), in females 171–185 ($\bar{x} = 178.0 \pm 9.9$; $N = 2$), no keeling. Cloacal plate divided. Subcaudal scales 31–43 ($\bar{x} = 37.6 \pm 3.7$; $N = 12$), in males 34–43 ($\bar{x} = 38.5 \pm 3.1$; $N = 10$), in females 31–35 ($\bar{x} = 33.0 \pm 2.8$; $N = 2$), paired. Total body scales 199–221 ($\bar{x} = 206.9 \pm 7.1$; $N = 11$), in males 199–217 ($\bar{x} = 205.8 \pm 5.9$; $N = 10$), in females 203–221 ($\bar{x} = 212.0 \pm 12.7$; $N = 2$). Subcaudal ratio 0.153–0.205 ($\bar{x} = 0.183 \pm 0.017$; $N = 11$), in males 0.171–0.205 ($\bar{x} = 0.189 \pm 0.012$; $N = 8$), in females 0.153–0.158 ($\bar{x} = 0.156 \pm 0.004$; $N = 2$). Sexual dimorphism detected for subcaudal ratio (Student's t-test $P = 0.00018$).

Head scalation (Fig. 5). Rostral enlarged, inflated, triangular in dorsal profile, curved onto upper surface of snout, in contact with first supralabial, nasal, and internasals. Posterior suture of rostral obtuse angled, "gull-wing" shaped in dorsal profile. Condition of nasal variable, completely divided (5/9 specimens), partially divided above (UMMZ 182640) or below nostril (CIB-CAS 102876, CIB 9968), or undivided (CAS 18005; holotype). Nostril positioned in the anterior edge of the nasal when com-

Figure 5. Head scalation of *Oligodon ornatus*. **A1–C1.** Dorsal view; **A2–C2.** Lateral view; **A3–C3.** Ventral view. **A.** UMMZ 182640, adult male, from Nantou, Taiwan, China; **B.** CIB 78058, adult male, from Wuyishan, Fujian, China; **C.** CIB-CAS 102876, adult male, from Yizhang, Hunan, China. Photographs by J.L. Lee (**A**) and Y.H. Xu (**B, C**).

pletely divided; when partially divided, nostril positioned in the median part of the entire scale. Internasals trapezoidal, paired, entire scale 1.7–2.1 times wider than long (all head scale proportions $N = 5$ unless noted otherwise), each blocked from contacting anteriorly by suture with rostral. Anterior and posterior internasal sutures concave. Median internasal suture 1.4–2.1 times shorter than entire scale. Prefrontals subrectangular, paired, entire scale broad, 1.3–1.5 times wider than long. Median prefrontal suture 1.7–2.8 times shorter than entire scale, longer or shorter than median internasal suture. Supraoculars longer than wide, narrower than prefrontals, posterior edge wider than anterior edge. Frontal large, pentagonal, shield shaped, longer than wide, 1.1–1.2 times longer than median parietal suture. Anterior frontal suture angled, positioned in front of eye sockets. Posterior vertex of frontal bordering parietal broad acute to weak obtuse angle (90–104°). Parietals large, subrectangular, paired, in broad contact, entire scale 1.0–1.3 times longer than frontal. Parietal suture bordering supraocular and frontal weak obtuse angle (113–130°), ray oriented posterolaterally. Median parietal suture shorter or equal to width of entire scale. Parietals surrounded by 7–10 scales ($N = 5$; excluding postoculars). Loreal absent. Preocular 1/1, rectangular, higher than long. Presubocular absent. Postoculars 2/2, rectangular, higher than long, uppermost scale slightly larger. Temporals usually 2+2 (8/11 specimens). One specimen (UMMZ 182640) with fused anterior and posterior temporal rows, resulting in scale formula of 2+1/1+1. Another specimen (CIB 9970) with fused posterior temporal row present, leading to a 2+1 temporal formula. The holotype of *Simotes musyi* (NHMB unnumbered) has a fusion between the temporolabial and the fifth supralabial, resulting in a 1+2 temporal formula on each side of the head. Lower anterior temporal broad in all specimens, diamond shaped, present as "temporolabial" scale leading to narrow contact between fifth and sixth supralabial. Supralabials 6/6, in one specimen 5/6 (UMMZ 182640); first scale smallest, fifth and sixth scale largest. First supralabial contacts nasal, second contacts nasal, prefrontal and preocular, third contacts preocular, third+fourth contact orbit, fifth+sixth contact lower temporals. One specimen with second+third supralabials contacting orbit on left side of head (UMMZ 182640). Infralabials 6/6 (10/12 specimens), rarely 7/7 (uncataloged specimen fide. Gong and He 2008) or 6/7 (SYS r001297). First pair of infralabials in contact at midline, second scale smallest, fourth scale largest. First four scales contact anterior chin shields. Anterior chin shields subrectangular, larger than posterior. Posterior chin shields also subrectangular, in contact at midline for half their length, suture bordering gulars concave. Mental groove poorly defined, present between first infralabials and posterior chin shields.

Dentition. Maxillary teeth 7–8, blade-like, the first is the smallest, increasing in size posteriorly (CAS 18005; ANU ZR25014). Zhao (2006) recorded a range of 7–9 maxillary teeth, but the specimens on which this description was based include material from Sichuan, Guangxi, and Hunan, which may be misidentified.

Coloration in life (Fig. 6). In life, dorsal surface of the body light brown. A broad, paravertebral stripe present followed by narrower lateral stripe on each side of body, both brown, extending from nape to tail. Paravertebral stripes positioned on dorsal scale rows 6–7, each 2.0–2.5 scales wide; lateral stripe between dorsal scale

Figure 6. *Oligodon ornatus* in life (unvouchered adult male from Wuyishan, Fujian, China). **A.** Dorsolateral view; **B.** Ventral view; **C.** Dorsal view of the head; **D.** Lateral view of the head; **E.** Ventral view of the head. Photographs by B.Q. Zhu.

rows 3–4, each 0.5–1.0 dorsal scales wide. One narrow middorsal line engulfed between paravertebral stripes, same color as remaining body. 8–10 transverse body bands ($\bar{x} = 8.8 \pm 0.9$; $N = 11$), 1–3 on tail ($\bar{x} = 1.8 \pm 0.6$; $N = 11$); total bands 10–12 ($\bar{x} = 10.7 \pm 0.7$; $N = 12$). Medial portion of each band is brown and lighter than the surrounding edges, which are typically dark brown to black. Some specimens exhibit secondary bands or spots concentrated middorsally or paravertebrally, contributing to a more complex dorsal pattern. Dorsal surface of head light brown or grayish brown marked with three distinct markings across the head and neck (ocular bar, temporal streak, nuchal chevron), each dark brown or reddish brown. Apex of ocular bar begins at the posterior edge of rostral and extends across internasals, prefrontals, supraoculars, and anterior margin of the frontal, then descends through the eye to partially cover the supralabials. Temporal streak starts near middle of the head and typically extends obliquely downward from the anterior and posterior temporals to the posterior part of the head, although in some specimens this streak may break into several irregular markings. Nuchal chevron forms an arrow or heart-shaped marking, beginning on the median portion of the parietals and continuing onto the nape. Ventral surface of head is white, scattered with irregular black markings. Underside of body also white with small subrectangular black blotches present on the lateral edges of ventral scales. Blotches are normally arranged at alternating intervals of one or two ventral scales but may be continuous or merge together. A red midventral streak runs between the dark blotches, extending from the anterior portion of the venter to the cloaca. Ventral surface of tail same color and blotch pattern as body, but red midventral streak typically fainter or absent, particularly towards the tail tip.

Coloration in preservative (Fig. 7). In preservative, ground color fades to pale brown on the dorsum and creamy white on the venter. Red midventral streak is no longer visible, but the dark dorsal bands and ventral blotches remain distinct.

Description of hemipenis (Fig. 8). The description is based on the fully everted left hemipenis of the adult male specimen QHU R2024047. When fully everted, the hemipenis is slender and columnar, extending to the 8th subcaudal scale. The asulcate side is relatively flat and wide, while the sulcate side is narrower and protrudes outward in an arched form. The total length is 15.12 mm, and the maximum width is 5.07 mm. Both sulcate and asulcate surfaces are densely covered with keratinized spines, which are arranged in approximately 16 rows that slope oblique-

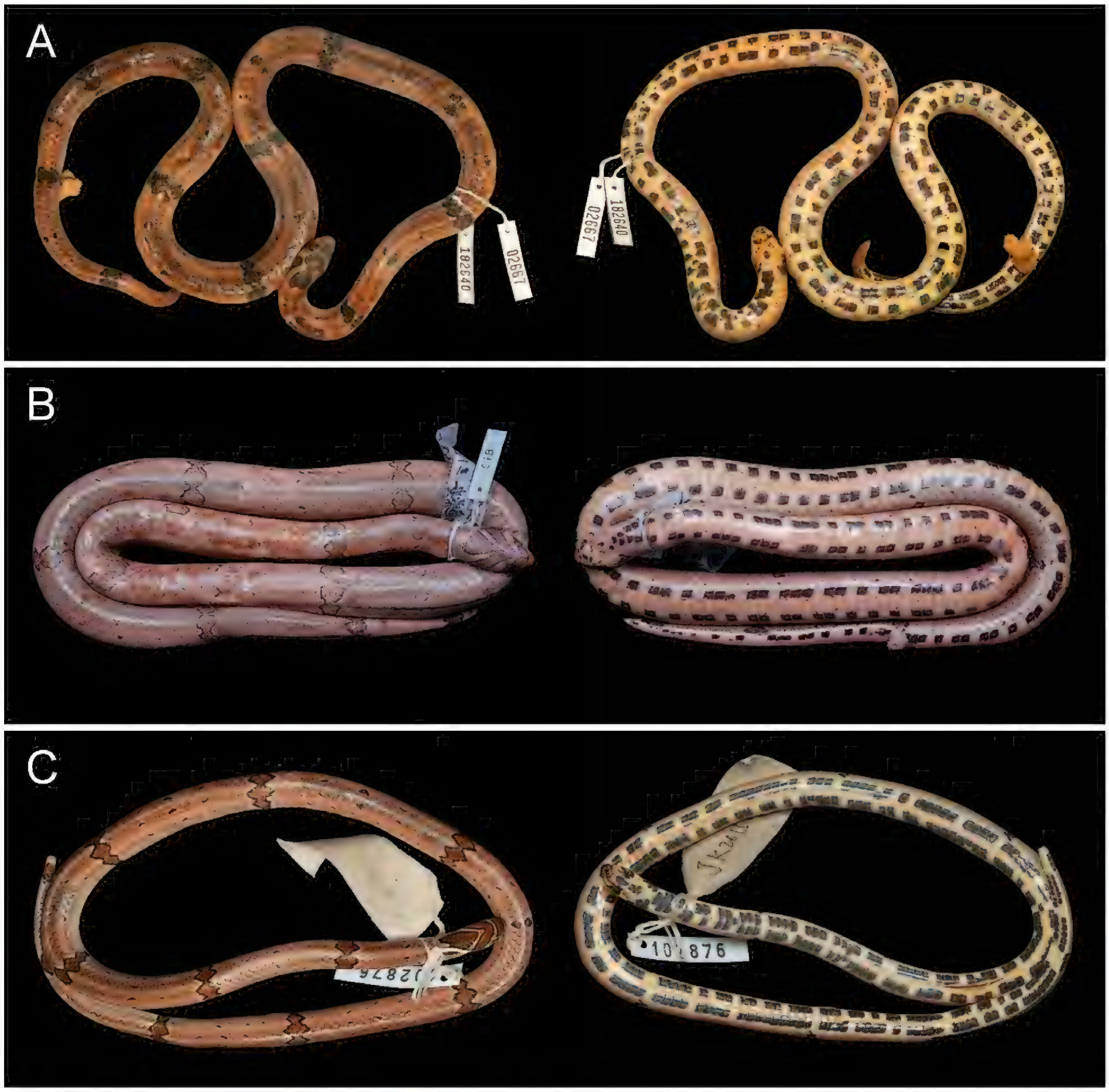

Figure 7. Preserved specimens of *Oligodon ornatus*. **A.** UMMZ 182640, adult male, from Nantou, Taiwan, China; **B.** CIB 78058, adult male, from Wuyishan, Fujian, China; **C.** CIB-CAS 102876, adult male, from Yizhang, Hunan, China. Photographs by J.L. Lee (**A**) and Y.H. Xu (**B, C**).

ly downward toward both sides from the midline of each surface; basal hook absent. The proximal one-eighth of the organ is smooth, followed by a dense region of large, relatively uniform, and laterally compressed spines. These gradually decrease in size beginning around the distal one-third. The central third of the apical surface bears spines, while the lateral thirds are smooth. The *sulcus spermaticus* is single and undivided, extending centripetally from the lateral base toward the distal tip. The sulcus lips are well-developed and slightly raised, walls smooth.

Distribution and natural history. *Oligodon ornatus* is primarily distributed in the mainland of eastern and southern China, including the provinces of Anhui, Jiangxi, Zhejiang, Fujian, Hunan, and Guangdong (Roux 1919; Pope 1935; Huang 1990; Chen 1991; Zhao et al. 1998; Gong and He 2008; this study); it is also widely distributed across the northern half of Taiwan Island, China (Van Denburgh 1909; Oshima 1910; Maki 1931; Kuntz 1963) (Fig. 1, Suppl. material 1: table S1). This species inhabits low to mid-elevation mountainous regions (209–1200 m asl.) in environments such as agricultural areas with cultivated crops (e.g., tea plantations or cornfields), bamboo forests, and broadleaf forests (Pope 1935; Zhao et al. 1998; Lee 2005; this study). According to available records, *O. ornatus* is oviparous and feeds on the eggs of other reptiles (Pope 1935; Shi and Zheng 1985; Zhao 2006; Gong and He 2008). Specifically, Pope (1935) recorded six reptile eggs in the stomach of a single specimen he collected. In addition, we observed that *O. ornatus* curls and raises its tail, exposing the vividly colored ventral surface when threatened and unable to escape. This behavior has been recorded previously in other

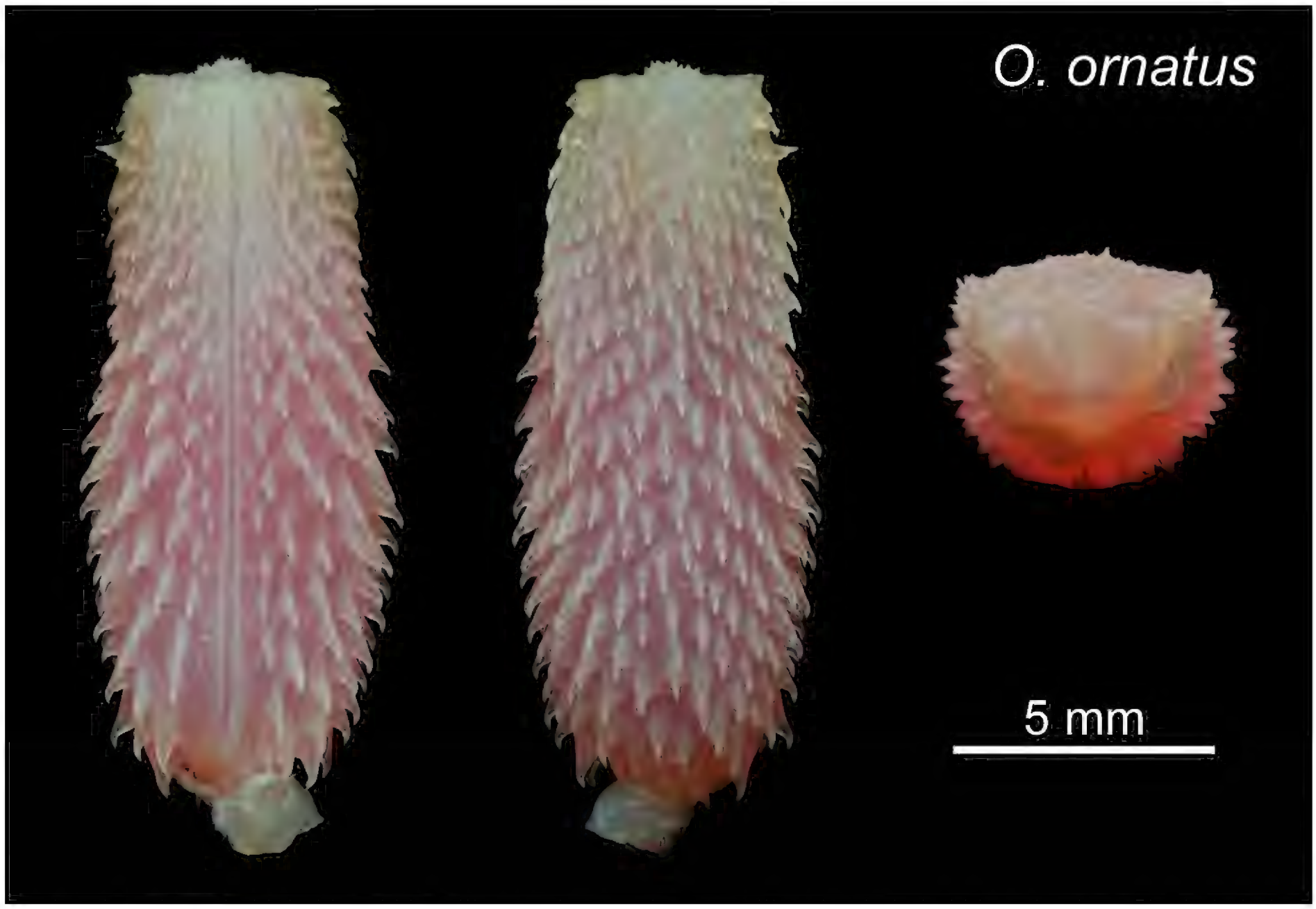

Figure 8. Sulcus side (left), asulcate side (middle), and apical side (right) of the hemipenis of *Oligodon ornatus* (QHU R2024047, adult male). Photographs by Y.H. Xu. Scale bar: 5 mm.

Oligodon and functions as a defensive display to intimidate or deter potential predators (Mori et al. 1992). This species displays marked aggressiveness when restrained, simultaneously attempting to bite and using its specialized tail tip to jab at perceived threats.

Conservation status. *Oligodon ornatus* was previously assessed as Least Concern (LC) on the IUCN Red List (Rao et al. 2024). Our updated and verified distributional data indicate that, although the species remains broadly distributed across eastern and southern China, its confirmed modern range is more restricted than historical records suggest. Nevertheless, there is no evidence of population decline, habitat deterioration, or severe fragmentation. GeoCAT analysis yielded an EOO of 631,670.5 km^2 and an AOO of 52,500.0 km^2. As the species does not meet the thresholds for a threatened category under criteria B or D, we recommend that *O. ornatus* be retained as LC.

Oligodon lungshenensis Zheng & Huang in Huang, Zheng and Fang 1978

Figs 9–12, Suppl. material 1: table S4

Longsheng Kukri Snake / 龙胜小头蛇 (Pinyin: Lóng Shèng Xiǎo Tóu Shé)

Synonymy. *Oligodon guizhouensis* – Li in Wu, Li, Xu, Dong and Liu (1979): 104.

Partial chresonymy. *Oligodon ornatus* (in part) – Zhao et al. (1986: 157); Zhao and Yang (1997: 238–239); Zhao (2002: 171); Li et al. (2020); Wu et al. (2023); Lee et al. (2024).

Type material. ***Holotype.*** • FNU 64099 (or NHMG 64099; see notes about holotype) (immature male), collector and collection date unknown. Type locality: Longsheng County, Guilin City, Guangxi Zhuang Autonomous Region, China.

Paratype. • NHMG 64100 (immature male), sharing the same collection data as the holotype, deposited in the NHMG.

Notes about holotype. In the original description, Huang et al. (1978) explicitly stated the holotype was deposited in Fujian Normal University and the paratype in the Natural History Museum of Guangxi Zhuang Autonomous Region (NHMG). However, both specimens were assigned NHMG catalogue numbers (Huang et al. 1978: 92). We made inquiries to the relevant institutions. At present, no archival records of *O. lungshenensis* or *O. ornatus* collected during the 20th century are retained in the collections of FNU; therefore, the holotype of *O. lungshenensis* was most likely lost.

Specimens examined (*N* = 11). China. Guangxi Zhuang Autonomous Region. • QHU R2024050 (Field NO. LFR 2024180; adult male), from Guilin City (approx. 25.275°N, 110.296°E), collected on 20 October 2024 by Y.H. Xu; • SYS r001529 (adult male), from Pinggui District, Hezhou Prefecture (24.293°N, 111.556°E, 345 m asl.), collected on 16 July 2016 by the team of Y.Y. Wang. **Guizhou Province.** • CIB F.201109039

(Field NO. TH1962; adult male), from Leigongshan, Leishan County, Qiandongnan Miao, and Dong Autonomous Prefecture (approx. 26.37°N, 108.16°E), collected on 24 September 2011 by the team of J.P. Jiang; • CIB 9963 (adult male), collected in August 1976, share the same locality as CIB F.201109039; • ANU ZR24115 (adult female), from Fangxiang Town, Leishan County, Qiandongnan Miao, and Dong Autonomous Prefecture (26.4192°N, 108.2367°E, 1098 m asl.), collected in August 2024 by T.R. Zhang; • QHU R2025048 (Field NO. LFR 2025226; adult female), collected on 26 September 2025 by the team of L.F. Peng, shares the same locality as ANU ZR24115. **Hunan Province.** • QHU R2024048 (Field NO. LFR 2024098; adult male), from Yongzhou City (approx. 26.45°N, 111.39°E), collected on 10 July 2024 by the team of L.F. Peng; • QHU R2025057 (Field NO. LFR 2025109; adult male), collected on 09 June 2025 by the team of L.F. Peng, shares the same locality as QHU R2024048; • ANU ZR24103 (adult female) and • ANU ZR240104 (adult male), from Longshan Forest Park, Lianyuan City, Loudi City (27.5033°N, 111.7465°E, 1046 m asl.), collected in 2024 by T.R. Zhang; • QHU R2025049 (Field NO. LFR 2025227; adult male), from Longshan forest park, Lianyuan City, Loudi City (27.5033°N, 111.7465°E, 1046 m asl.), collected on 12 September 2025 by the team of L.F. Peng.

Other reported specimens (*N* = 24). China. Chongqing Municipality. • CTS 20090624 (adult female), from Shuishi Township, Qianjiang District (29.2348°N, 108.6873°E; 1000 m asl.), collected on 24 June 2009 by Zhishen Fei, reported by Luo et al. (2010). • KIZ YPX18635, sex and collection data unknown, from Qianjiang District (approx. 29.53°N, 108.77°E), reported by Wu et al. (2023). **Guizhou Province.** • ZMU 7600060 (adult male), the holotype of *O. guizhouensis*, from Yongle Town, Leishan County, Qiandongnan Miao, and Dong Autonomous Prefecture (26.2257°N, 108.2211°E; 630 m asl.); • ZMU 770272 (adult male), • ZMU 770273 (adult male), • ZMU 770275 (adult male), • ZMU 750159 (adult female), • ZMU 770274 (adult female), and • ZMU 770271 (adult female), from Chishui City, Zunyi City (approx. 28.36°N, 105.78°E); and • ZMU 7610418 (adult female), • ZMU 7610419 (juvenile female), • ZMU 7610421 (juvenile female), and • ZMU 770364 (juvenile female), from Leishan County, Qiandongnan Miao and Dong Autonomous Prefecture (approx. 26.37°N, 108.16°E), all of which are designated as paratypes of *O. guizhouensis*. These 11 specimens were reported by Wu et al. (1979). • TRU R201107001 (adult female), from Fodingshan Nature Reserve, Shiqian County, Tongren City (27.3371°N, 108.1601°E; 619 m asl.), collected on 07 July 2011, reported by Ran et al. (2012). **Hubei Province.** • XDSNR 0011 (adult male), from Xingdoushan Nature Reserve, Enshi City (30.067°N, 109.233°E; 1179 m asl.), collected on 12 August 2022, reported by Dong et al. (2023). **Hunan Province.** • CWNU unnumbered (adult male), from Mangshan National Nature Reserve, Chenzhou City (24.967°N, 112.867°E, 1000 m asl.), collected July 2008, reported by Yuan et al. (2010). • HNNU 920897 (adult female), from Shimen County, Changde City (approx. 29.58°N, 111.38°E); • HNNU 810732 (adult female), • HNNU 810731 (juvenile male), • HNNU 590046 (juvenile male) from Dayong, Zhangjiajie City (approx. 29.12°N, 110.48°E); • HNNU 590014 (adult female), from Jiangyong County, Yongzhou City (approx. 25.27°N, 111.34°E); • HNNU 590046 (adult female), from Cili County, Zhangjiajie City (approx. 29.43°N, 111.13°E). These 6 specimens were reported by Shen et al. (2014). • HS11016 (now ANU HS11016), sex and collection data unknown, from Yongzhou City (approx. 26.45°N, 111.39°E), reported by Li et al. (2020). **Sichuan Province.** • YBU 240279 (adult female), from Xianlong Village, Xiantan Town, Hejiang County, Luzhou City (106.2758°N, 28.6517°E; 696 m asl.), collected 22 June 2023, reported by Liu et al. (2025). Literature data from reported specimens are mentioned in the description. For electronic records, refer to Suppl. material 1.

Revised diagnosis. A medium sized *Oligodon*, tail moderately long (TailLR 0.106–0.147; in males 0.114–0.147; in females 0.106–0.133). Dorsal scales in 15–15–15 rows, all smooth, no reductions. Ventral scales 163–186, no dimorphism (163–185 in males, and 167–186 in females), no keeling. Cloacal plate divided. Subcaudals 31–40 (31–40 in males, 31–35 in females), paired. Total body scales 198–218 (198–215 in males, 201–218 in females). Subcaudal ratio 0.142–0.188, no dimorphism (in males 0.148–0.188, in females 0.142–0.172). Maxillary teeth 8, posterior three teeth slightly enlarged and blade-like. Internasals absent, fused with prefrontals. Loreal absent, preocular 1, presubocular absent, postoculars 2 (rarely 1), temporals 2+2 (rarely 2+1). Temporolabial scale present. Supralabials 6 (rarely 5), 3rd–4th in contact with the eye (rarely 2nd–3rd in contact). Infralabials 6–7 (rarely 5), first 1–4 in contact with anterior chin shields (rarely 1–3). Dorsal surface light brown or grayish brown with a broad brown paravertebral stripe and a narrower lateral stripe on either side of body, both extending from nape to tail. Middorsal line between paravertebral stripes, same color as remaining body. A total of 9–14 irregular dorsal bands present (7–11 on body, and 1–3 on tail), some specimens exhibiting secondary bands or spots concentrated along the middorsal or paravertebral regions. Median portions of each band brown, edges normally dark brown or black. Head markings include ocular bar, temporal bar, and nuchal chevron. Ventral surface white with lateral series of black alternating rectangular blotches on ventral scales and a broad red midventral stripe in life. Hemipenis unilobed, simple sulcus spermaticus, spines gradually decreasing in size by midpoint of organ, and absent on distal one-fifth of organ and apical surface.

Description and variation. The main morphological characteristics of *O. lungshenensis* are summarized in Suppl. material 1: table S4, based on newly examined specimens in this study (*N* = 11) and previous reports by Huang et al. (1978), Wu et al. (1979), Zhao et al. (1986),

Yuan et al. (2010), Luo et al. (2010), Ran et al. (2012), Dong et al. (2023), and Liu et al. (2025) ($N = 17$).

Body slender, subcylindrical. Head oblong, slightly distinct from neck. Snout elongate, narrowing in width in dorsal profile, slightly truncate in lateral profile. Eyes moderate relative to head, pupil round. Nostrils small, subelliptical, pointed laterally. Tail short to moderate, tapering gradually to sharp pointed tip. Largest specimen an adult female (ANU ZR24115) measuring 612 mm SVL and 79 mm TailL. Largest male (uncatalogued specimen reported by Zhao et al. 1986) 550 mm SVL, 95 mm TailL. Head measurements ($N = 11$ unless noted otherwise) as follows: HeadL 12.8–17.3 mm ($N = 12$), HeadW 8.0–10.9 mm ($N = 12$), SnoutL 4.1–6.1, EyeD 2.0–3.1 mm, IOD 5.5–6.7 mm ($N = 10$), IND 3.6–4.9 mm, FrontalL 3.9–5.9 mm, FrontalW 3.5–5.1 mm. TailLR 0.106–0.147 ($\bar{x} = 0.126 \pm 0.012$; $N = 28$), in males 0.114–0.147 ($\bar{x} = 0.132 \pm 0.012$; $N = 14$), in females 0.106–0.133 ($\bar{x} = 0.120 \pm 0.009$; $N = 14$), sexual dimorphism present (Student's t-test $P = 0.00468$). HeadW/HeadL 0.52–0.76 ($N = 12$), SnoutL/HeadL 0.27–0.41 ($N = 11$), EyeD/SnoutL 0.36–0.51 ($N = 11$), EyeD/HeadL 0.13–0.21 ($N = 11$), FrontalL/FrontalW 1.02–1.30 ($N = 11$).

Body scalation. Dorsal scales in 15–15–15 rows, all smooth with no reductions. Ventral scales 163–186 ($\bar{x} = 171.0 \pm 5.3$; $N = 28$), in males 163–185 ($\bar{x} = 169.7 \pm 5.0$; $N = 14$), in females 167–186 ($\bar{x} = 172.4 \pm 5.5$; $N = 14$), no keeling. Cloacal plate divided. Subcaudal scales 31–40 ($\bar{x} = 34.0 \pm 2.5$; $N = 28$), in males 31–40 ($\bar{x} = 34.8 \pm 2.9$; $N = 14$), in females 31–35 ($\bar{x} = 32.6 \pm 1.4$; $N = 14$), paired. Total body scales 198–218 ($\bar{x} = 206.4 \pm 5.5$; $N = 28$), in males 198–215 ($\bar{x} = 205.9 \pm 5.1$; $N = 14$), in females 201–218 ($\bar{x} = 207.1 \pm 5.9$; $N = 14$). Subcaudal ratio 0.142–0.188 ($\bar{x} = 0.163 \pm 0.011$; $N = 28$), in males 0.148–0.188 ($\bar{x} = 0.169 \pm 0.012$; $N = 14$), in females 0.142–0.172 ($\bar{x} = 0.157 \pm 0.008$; $N = 14$). Sexual dimorphism detected for subcaudal scales (Student's t-test $P = 0.01358$) and subcaudal ratio (Student's t-test $P = 0.00609$).

Head scalation (Fig. 9). Rostral enlarged, inflated, triangular in dorsal profile, curved onto upper surface of snout, in contact with first supralabial, nasal and prefrontals. Posterior suture of rostral obtuse angled, "gull-wing" shaped in dorsal profile. Condition of nasal variable, completely divided (in CIB F.201109039 and ANU ZR24115), partially divided above (left side of head in QHU 2024050) or below nostril (4/11 specimens), or undivided (4/11 specimens + right side of head in QHU 2024050). Nostril positioned in the anterior edge of the nasal when completely divided; when partially divided, nostril positioned in the median part of the entire scale. Internasals absent, fused with prefrontals. Prefrontals subrectangular, paired, entire scale broad, 1.0–1.1 times wider than long. Anterior and posterior prefrontal sutures concave. Median prefrontal suture 2.2–2.5 times shorter than entire scale. Supraoculars longer than wide, narrower than prefrontals, posterior edge wider than anterior edge. Frontal large, pentagonal, shield shaped, longer than wide, 1.3–1.5 times longer than median parietal suture. Anterior frontal suture angled, positioned in front of eye sockets. Posterior vertex of frontal bordering parietal broad acute to weak obtuse angle (87–102°). Parietals large, subrectangular, paired, in broad contact, entire scale 1.0–1.1 times longer than frontal. Parietal suture bordering supraocular and frontal weak obtuse angle (121–130°), ray oriented posterolaterally. Parietals surrounded by 7–9 scales ($N = 5$; excluding postoculars). Loreal absent. Preocular 1/1, rectangular, higher than long. Presubocular absent. Postoculars 2/2 (19/28 specimens), rarely 1/1 (7/28 specimens) or 1/2 (2/28 specimens; in ANU ZR24104 and QHU R2025057), rectangular, higher than long, uppermost scale slightly larger. Temporals 2+2. In two specimens (QHU 2024048 and XDSNR0011 fide. Dong et al. 2023) posterior temporals fused, resulting in scale formula of 2+1. Lower anterior temporal broad, diamond shaped, present as "temporolabial" scale leading to narrow contact between fifth and sixth supralabial. Supralabials 6/6, in one specimen 5/5 (YBU 240279 fide. Liu et al. 2025); first scale smallest, fifth and sixth largest. First supralabial contacts nasal, second contacts nasal, prefrontal and preocular, third contacts preocular, third+-fourth contact orbit, fifth+sixth contact lower temporals. In two specimens the second+third supralabials contact orbit (YBU 240279 fide. Liu et al. 2025; ANU ZR24115 on right side of head). Infralabials 7/7 (9/17 specimens) or 6/6 (8/17 specimens), rarely 7/6 (CIB F.201109039) or 5/6 (QHU R2025048). First pair of infralabials in contact at midline, second scale smallest, fourth scale largest. First four infralabials contact anterior chin shields (8/11 specimens), exceptionally 3/4 (SYS r001529), 4/3 (CIB F.201109039), or 3/3 (QHU R2025048). Anterior chin shields subrectangular, larger than posterior. Posterior chin shields also subrectangular, in contact at midline for half their length, suture bordering gulars concave. Mental groove poorly defined, present between first infralabials and posterior chin shields.

Dentition. Maxillary teeth 8, enlarged and blade-like, increasing in size posteriorly (based on QHU R2024048, R2024050, R2025057 and R2025049). Wu et al. (1979) and Zhao (2006) recorded the same tooth counts in their material.

Coloration in life. In life (Fig. 10), dorsal surface light brown to grayish brown. A broad, paravertebral stripe present followed by narrower lateral stripe on each side of body, both brown, extending from nape to tail. Paravertebral stripes positioned on dorsal scale rows 6–7, each 2.0–2.5 scales wide; lateral stripe between dorsal scale rows 3–4, each 0.5–1.0 dorsal scales wide. One narrow middorsal line engulfed between paravertebral stripes, same color as remaining body. 7–11 transverse body bands ($\bar{x} = 8.7 \pm 0.8$; $N = 26$), 1–3 on tail ($\bar{x} = 2.4 \pm 0.7$; $N = 26$); total bands 9–14 ($\bar{x} = 11.3 \pm 1.2$; $N = 28$). Median portion of each band brown, lighter than the surrounding edges, which are typically dark brown or black. Some specimens exhibit secondary banding or spotting across body, concentrated middorsally or paravertebrally contributing to a more complex dorsal pattern (YBU

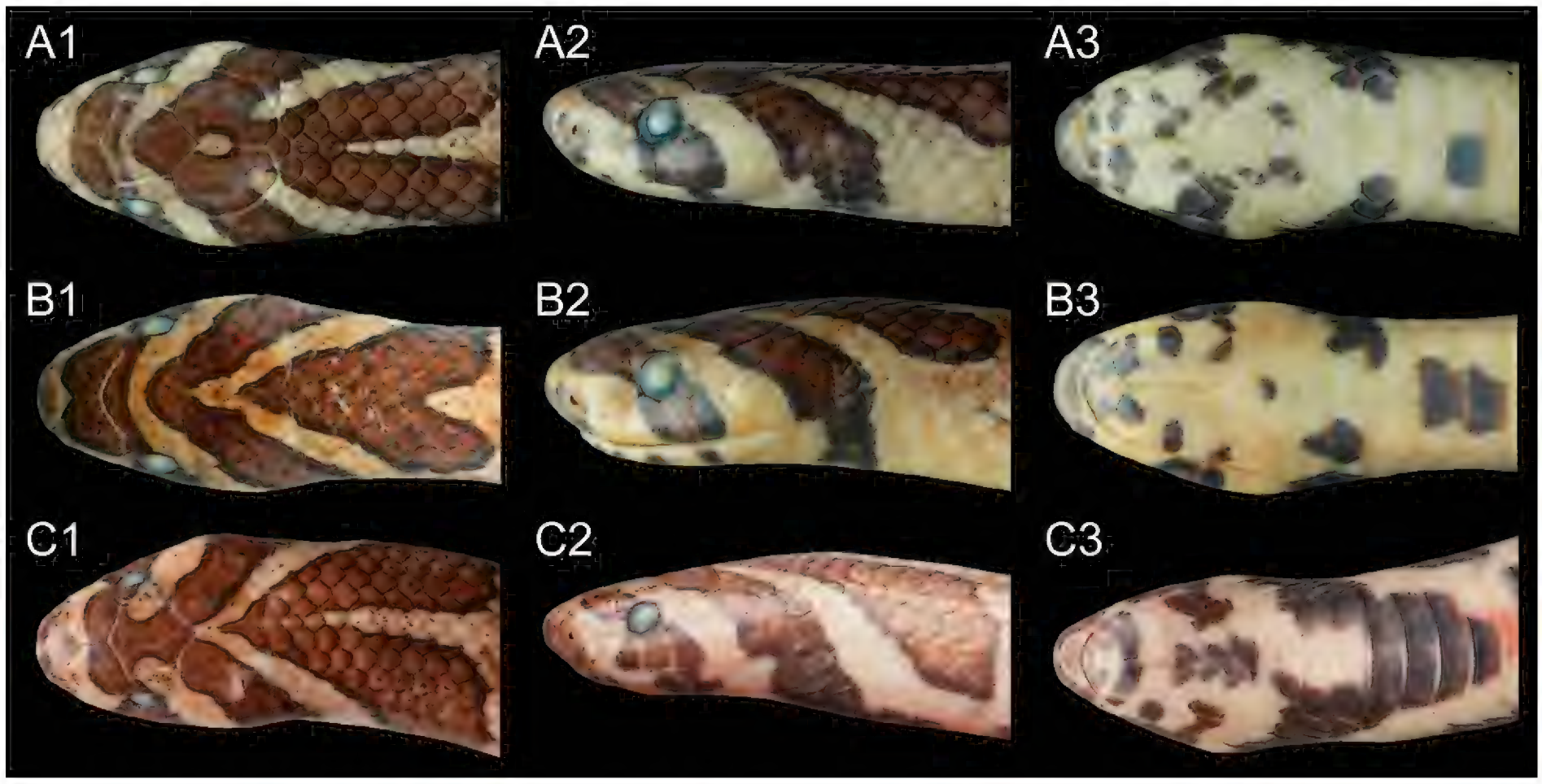

Figure 9. Head scalation of *Oligodon lungshenensis*. **A1–C1.** Dorsal view; **A2–C2.** Lateral view; **A3–C3.** Ventral view. **A.** QHU R2024050, adult male, from Guilin, Guangxi, China; **B.** SYS r001529, adult male, from Hezhou, Guangxi, China; **C.** CIB F.201109039, adult male, from Leigongshan, Guizhou, China. Photographs by Y.H. Xu.

Figure 10. *Oligodon lungshenensis* in life (QHU R2024050, adult male, from Guilin, Guangxi, China). **A.** Dorsolateral view; **B.** Ventral view; **C.** Dorsal view of the head; **D.** Lateral view of the head; **E.** Ventral view of the head. Photographs by Y.H. Xu.

240279 fide. Liu et al. 2025: Fig. 1). Dorsal surface of the head light brown to grayish brown, marked by ocular bar, temporal streak and nuchal chevron. All three head markings brown or reddish brown, slightly paler medially, bordered by dark brown. Ocular bar has its apex positioned at the posterior edge of the rostral, extending across internasals, prefrontals, supraoculars, and anterior margin of frontal, descending through eye to partially covering first 2–3 supralabials. Apex of temporal streak arises near middle of head, extending obliquely across temporals to the posterior end of the head. Nuchal chevron arrow-shaped or heart-shaped, starting at median edge of parietals and extending onto nape. Ventral surface of head white, scattered with irregular black blotches. Underside of body also white, small subrectangular black blotches present across lateral edges of ventral scales. These ventral blotches are typically arranged at alternating intervals of 1–2 scales, though they can be continuous in some examples. One red midventral streak present between dark blotches extending from throat to cloaca. Underside of tail same coloration and pattern as body, though red midventral streak may become faint or absent, particularly near the tail tip.

Coloration in preservative (Fig. 11). In preservative, ground color fades to pale brown on the dorsum and creamy white on the venter. The red midventral streak is no longer visible, but the dark dorsal bans and ventral blotches remain distinct. In addition, the black ventral blotches in specimen CIB F.201109039 enlarge in the mid- to posterior body region and subsequently merge,

Figure 11. Preserved specimens of *Oligodon lungshenensis*. **A.** QHU R2024050, adult male, from Guilin, Guangxi, China; **B.** SYS r001529, adult male, from Hezhou, Guangxi, China; **C.** CIB F.201109039, adult male, from Leigongshan, Guizhou, China. Photographs by Y.H. Xu.

causing the entire central portion of the ventral surface in this region to become uniformly black (Fig. 11C).

Description of hemipenis. (Fig. 12). Description based on everted left organ of adult male specimen QHU R2024050. When fully everted, hemipenis thin, short, and cylindrical, elliptical in cross-section, and extending to the 9th subcaudal scale. Hemipenial total length 14.55 mm, maximum width 5.05 mm. Both sulcate and asulcate surfaces are densely covered with spines, which are arranged in approximately 15 faintly defined rows; basal hooks are absent. First sixth of hemipenis nude, followed immediately by large, keratinized spines restricted to proximal half. Width of hemipenis narrows slightly in a transverse manner past midpoint. Spines gradually decrease in size after midpoint and disappear completely at the distalmost fifth of the organ near the apex. The apical surface is predominately smooth with occasional scattered small papillae-shaped calyces. The *sulcus spermaticus* is simple and non-bifurcate, extending centripetally from the base to the apex. Sulcus lips well-developed, slightly raised, walls smooth.

Distribution and natural history. This species is endemic to south to southwest China, where it is known from Chongqing Municipality, Guangdong Province, Guangxi Zhuang AR, Guizhou Province, Hunan Province, Hubei Province, and Sichuan Province (Huang et al. 1978; Wu et al. 1979; Zhao et al. 1986; Yuan et al. 2010; Luo et al. 2010; Ran et al. 2012; Dong et al. 2023; Liu et al. 2025; this study) (Fig. 1, Suppl. material 1: table S1). The record from Sichuan Province was first reported from Miyi County, Panzhihua City, and was identified as *Oligodon ornatus* (Zhao et al. 1986; Zhao and Yang 1997; Zhao 2002). However, the described specimen was noted to lack internasal scales, a diagnostic trait of *O. lungshenensis*. This observation is also consistent with the more westerly distribution of *O. lungshenensis* compared to *O. ornatus*. All known localities are situated at mid-to-high elevations (between 619–1500 m asl.) in habitats characterized by evergreen broadleaf forests (Huang et al. 1978; Wu et al. 1979; Zhao et al. 1986; Zhao 2006; Yuan et al. 2010; Luo et al. 2010; Ran et al. 2012; Dong et al. 2023; Liu et al. 2025; this study). Zhao (2006) reported a female specimen of *Oligodon lungshenensis* from Guizhou Province containing five eggs, confirming that the species is oviparous. The same study also noted that *O. lungshenensis* primarily feeds on reptile eggs, but no specific predator-prey observations have been documented. When threatened and unable to escape, *O. lungshenensis* exposes its vividly colored ventral surface by curling and raising its tail. This species also displays marked aggressiveness when handled and will simultaneously attempt to bite and use its tail tip to jab at perceived threats.

Etymology. Named after the type locality in Longsheng County, Guilin City, Guangxi. Treated as a Latinized adjective in nominative case. Its Chinese common name is “

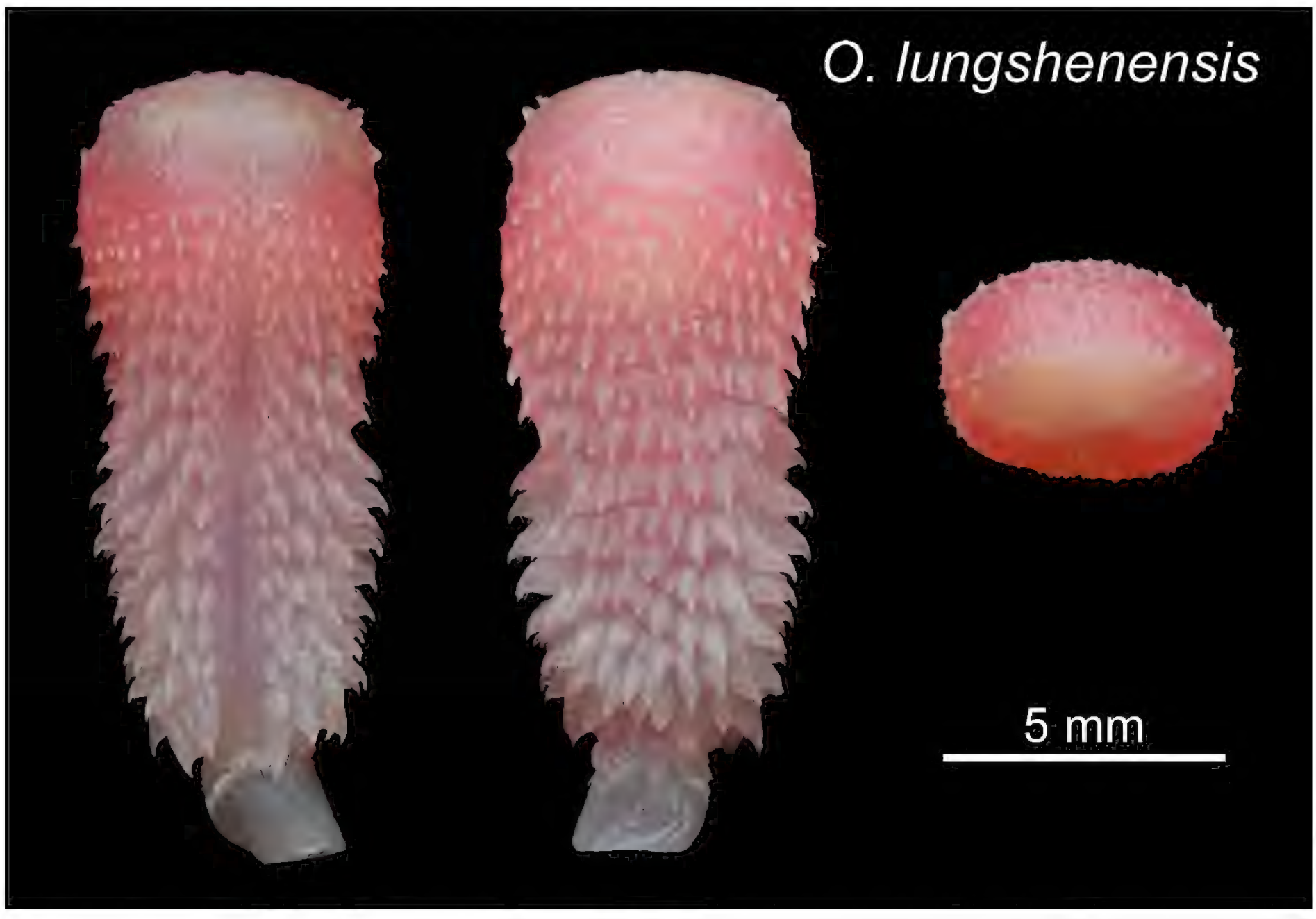

Figure 12. Sulcus side (left), asulcate side (middle), and apical side (right) of the hemipenis of *Oligodon lungshenensis* (QHU R2024050, adult male). Photographs by Y.H. Xu. Scale bar: 5 mm.

龙胜小头蛇" (Pinyin: Lóng Shèng Xiǎo Tóu Shé). In addition, since this species has long lacked a formal English name, we propose the name "Longsheng Kukri Snake" based on its type locality and specific epithet.

Conservation status. *Oligodon lungshenensis* was previously assessed as Near Threatened (NT) on the IUCN Red List (Zhou et al. 2012). Our updated and verified distributional data indicate that the species has a broader range than previously assumed. GeoCAT analysis yielded an EOO of 369,331.6 km^2 and an AOO of 42,500.0 km^2. Accordingly, we recommend that the conservation status of *O. lungshenensis* be revised to Least Concern (LC).

Oligodon bivirgatus Qian, Qi, Shi, Lu, Jenkins, Mo & Li, 2021

Figs 13–18, Suppl. material 1: table S4

Double Striped Kukri Snake / 双线小头蛇 (Pinyin: Shuāng Xiàn Xiǎo Tóu Shé)

Chresonymy. *Oligodon ornatus* – Kadoorie Farm and Botanic Garden (2001): 15.

Type material. ***Holotype.*** • SYNU 1907027 (adult female), collected on 13 July 2019 by T.Y. Qian and M.H. Huang. Type locality: Shangxi Nature Reserve, Hainan Province, China (18.834167°N, 110.130833°E; 319 m asl.).

Paratype. • SYNU 1808001 (adult female), collected on 17 August 2018 by P.P. Li, T.Y. Qian and M.H. Huang from the same valley as the holotype (18.833611°N, 110.130556°E; 317 m asl.).

Specimens examined (*N* = 3). China. Hainan Province. • QHU R2024049 (Field NO. LFR 2024108; adult male), from Diaoluoshan, Lingshui Li Autonomous County, (18.6735°N, 109.8776°E; 510 m asl.), collected on 29 May 2024 by C.X. Liao; • SYS r002952 (iNaturalist 284182249; adult male), a road-killed specimen, from Jianfengling National Forest Park, Ledong Li Autonomous County (18.7386°N, 108.8623°E; 837 m asl.), collected on 23 May 2025 by H.M. Song and S. Qi; • iNaturalist 298113949 (adult male), from Tianchi Village, Jianfengling National Forest Park, Ledong Li Autonomous County (18.73670°N, 108.85386°E; 1042 m asl.), observed on 22 June 2025 by B. Genter, released back into the wild after measurement and photography.

Revised diagnosis. A medium sized *Oligodon*, tail moderate in relative length (TailLR 0.121–0.164; in males 0.136–0.164, in females 0.121–0.131). Dorsal scales in 15–15–15 rows, all smooth and no reductions. Ventral scales 150–176 (150–156 in males, 173–176 in females). Cloacal plate divided. Subcaudals 33–37 (33–37 in males, 34–37 in females), paired. Total body scales 184–211 (184–193 in males, 211 in females). Subcaudal ratio 0.161–0.192, strong dimorphism (0.179–0.192 in males, 0.161–0.175 in females). Maxillary teeth 8, posterior three teeth slightly enlarged and blade-like. Internasals separate from prefrontals. Loreal absent, preocular 1, presubocular absent, postoculars 2, and temporals 2+2. Temporolabial scale present. Supralabials 6, 3rd–4th in contact with the eye. Infralabials 7 (rarely 6), first four in contact with anterior chin shields. Dorsal surface light brown or reddish brown. Two narrow, dark brown paravertebral stripes running from nuchal chevron to tail and two indistinct lateral stripes along flanks. Head plain with three dark brown markings: an ocular bar, temporal bar, and nuchal chevron. Ventral surface typically white with a lateral series of black rectangular spots and an orange red midventral streak, but also orange red with small, and indistinct cream spots laterally along the anterior third of the body. Hemipenis unilobed, simple sulcus spermaticus, spines uniformly sized, and present across entire organ.

Description and variation. Based on Qian et al. (2021) and three newly examined specimens. The main morphological characters of the specimens used in this study are listed in Suppl. material 1: table S4. Body slender, subcylindrical, broader at midbody. Head oblong, slightly distinct from neck. Snout elongate, narrowing in width in dorsal view, slightly truncate in lateral view. Eyes moderate, pupil round. Nostrils small, subelliptical, pointed laterally. Tail moderate, tapering gradually to a sharp pointed tip. Adult SVL 358–404 mm, TailL 51–70 mm, TotalL 422–465 mm. Juveniles unknown. Largest specimen an adult female (SYNU 1907027) measuring 404 mm SVL and 61 mm TailL. Largest male (SYS r002952) measured 401 mm SVL and 63 mm TailL. Head measurements as follows (N = 4 unless stated otherwise): HeadL 14.1–14.2 mm (N = 2), HeadW 7.6–9.0 mm, SnoutL 4.3–5.1 mm, EyeD 2.1–2.3 mm, IOD 5.2–5.4 mm, IND 3.7 mm (N = 2), FrontalL 4.6 mm (N = 2), FrontalW 3.8 mm (N = 2). TailLR 0.121–0.164 ($\bar{x}$ = 0.141 ± 0.017; N = 5), in males 0.136–0.164 ($\bar{x}$ = 0.151 ± 0.014; N = 3), in females 0.121–0.131 ($\bar{x}$ = 0.126 ± 0.007; N = 2). HeadW/HeadL 0.54–0.63 (N = 2), SnoutL/HeadL 0.32–0.36 (N = 2), EyeD/SnoutL 0.43–0.50, EyeD/HeadL 0.16 (N = 2), FrontalL/W 1.21–1.29 (N = 2). The type series in Qian et al. (2021) had HeadL values of 12.9–16.8 mm measured "from snout tip to jaw angles", though it is unclear if the "jaw angles" refer to the posterior end of the dentary bone (as measured here) or the edge of the mouth. Ratios for these measurements as follows: HeadW/HeadL 0.54–0.60, SnoutL/HeadL 0.30–0.33, EyeD/HeadL 0.13–0.16.

Body scalation. Dorsal scales in 15–15–15 rows, all smooth, no reductions. Ventral scales 150–176 ($\bar{x}$ = 162.0 ± 11.7; N = 5), in males 150–156 ($\bar{x}$ = 154.0 ± 3.2; N = 3), in females 173–176 ($\bar{x}$ = 175.0 ± 2.1; N = 2), no keeling. Cloacal plate divided. Subcaudal scales 33–37 ($\bar{x}$ = 35.0 ± 1.8; N = 5), in males 33–37 ($\bar{x}$ = 35.0 ± 2.1; N = 3), in females 34–37 ($\bar{x}$ = 36.0 ± 2.1; N = 2), paired. Total body scales 184–211 ($\bar{x}$ = 198.4 ± 12.1; N = 5), in males 184–193 ($\bar{x}$ = 190.0 ± 5.2; N = 3), in females 211 ($\bar{x}$ = 211.0 ± 0.0; N = 2). Subcaudal ratio 0.161–0.192 ($\bar{x}$ = 0.179 ± 0.012; N = 5), in males 0.179–0.192 ($\bar{x}$ = 0.186 ± 0.006; N = 3), in females 0.161–0.175 ($\bar{x}$ = 0.168 ± 0.010; N = 2). Sexual dimorphism recorded for ventrals (Student's

t-test $P = 0.00338$) and total body scales (Student's t-test $P = 0.01980$).

Head scalation (Fig. 13). Rostral enlarged, inflated, triangular in dorsal profile, curved onto upper surface of snout, in contact with first supralabial, nasal, and internasals. Posterior suture of rostral obtuse angled, "gull-wing" shaped in dorsal profile. Nasal completely divided in type series (SYNU 1907027 and SYNU 1808001) or partially divided below nostril (QHU R2024049, iNaturalist 298113949). Nostril situated in the anterior edge of the nasal when completely divided; when partially divided, nostril lies in the median part of the entire scale. Internasals subrectangular, paired, entire scale 1.7–1.9 times wider than long (all head scale proportions $N = 2$ unless noted otherwise), each blocked from contacting anteriorly by suture with rostral. Anterior and posterior internasal sutures concave. Median internasal suture 2.2–2.3 times shorter than entire scale. Prefrontals present, subrectangular, paired, entire scale 1.2 times wider than long. Median prefrontal suture 2.1–2.4 times shorter than entire scale, longer than median internasal suture. Supraoculars longer than wide, narrower than prefrontals, posterior edge wider than anterior edge. Frontal large, pentagonal, shield shaped, longer than wide, 1.3–1.5 times longer than median parietal suture. Anterior frontal suture angled, positioned in front of eye sockets. Posterior vertex of frontal bordering parietal weak obtuse angle (91–98°). Parietals large, subrectangular, paired, in broad contact, entire scale 1.2 times longer than frontal. Parietal suture bordering supraocular and frontal weak obtuse angle (115–129°), ray oriented posterolaterally. Parietals surrounded by 9–10 scales ($N = 3$; excluding postoculars). Loreal absent. Preocular 1/1, rectangular, higher than long. Presubocular absent. Postoculars 2/2, rectangular, higher than long, uppermost scale slightly larger. Temporals 2+2. Lower anterior temporal broad, diamond shaped, present as "temporolabial" scale, resulting in narrow contact between fifth and sixth supralabial. Supralabials 6/6, first scale smallest, fifth and sixth scale largest. First supralabial in contact with nasal, second in contact with nasal, prefrontal and preocular, third contacts preocular, third and fourth in contact with the orbit, fifth and sixth scale contact anterior and posterior temporal row. Anterior chin shields larger than posterior pair. Infralabials 7/7 (6/6 in iNaturalist 298113949), first pair in contact at midline, second scale smallest, fourth scale largest. First four scales contact anterior chin shields. Anterior chin shields subrectangular, larger than posterior. Posterior chin shields also subrectangular, in contact at midline for half their length, suture bordering gulars con-

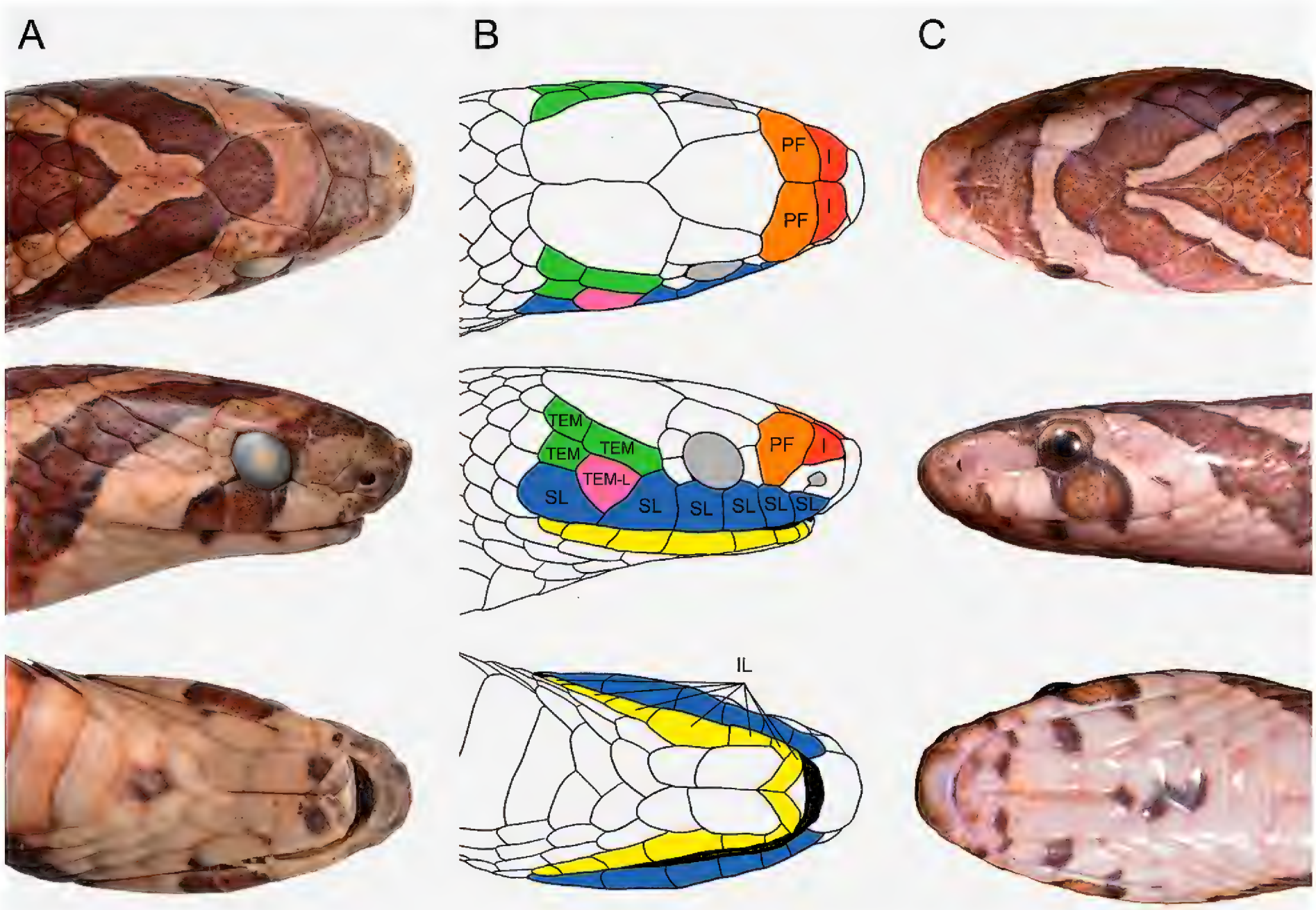

Figure 13. Head scalation photographs and drawings of *Oligodon bivirgatus*. **A, B.** Specimen QHU R2024049 (adult male, from Diaoluoshan, Hainan); **C.** SYNU 1907027 (holotype, adult female, from Shangxi Nature Reserve, Hainan). Notes: PF, prefrontal; I, internasal; IL, infralabials; SL, supralabials; TEM, temporals; TEM-L, temporolabial. Photographs and drawings by Y.H. Xu (**A, B**) and reproduced from Qian et al. (2021) (**C**).

cave. Mental groove poorly defined, present between first infralabials and posterior chin shields.

Dentition. Maxillary teeth 8 (N = 3), blade-like, anteriormost two teeth smallest, increasing in size posteriorly.

Coloration in life. In life, *Oligodon bivirgatus* exhibits two distinct color morphs. Dorsal ground color of typical morph pale brown to pale reddish-brown (Fig. 14; Qian et al. 2021). A pair of dark brown paravertebral stripes present extending from nape to tail tip, each on dorsal scale rows 6–7 and 0.5–1.5 scales wide. Middorsal space between stripes 2.5–3.0 dorsal scales wide. Dorsal surface of head light brown. Ocular bar, temporal streak and nuchal chevron all present, each brown, slightly pale medially, bordered by dark pigment. Ocular bar positioned at posterior edge of rostral, extending across internasals, prefrontals, supraoculars, and anterior margin of the frontal, descending through the eye to partially cover the margins of supralabials 3–5. Temporal bar arises near middle of head, extending obliquely downwards from the posterior median of the frontal through each parietal, upper anterior temporal and both posterior temporals before terminating at the lateral end of the nape. Nuchal chevron present as an arrow-shaped marking beginning on the median edge of the parietals before continuing occipitally across the nape. Lateral edges of nuchal chevron continue as paravertebral stripes down the remaining body. Underside of head cream or white, mental scale grayish brown. Scattered irregular dark brown spots on the edges of the first 1–4 infralabials, or medially along gular scales. Ventral surface of body cream or white, small subrectangular black blotches present at intervals of one or two ventral scales on their lateral edges, though they may be continuous in some areas. An orange red midventral streak runs between the dark blotches, extending from the anterior portion of the venter. Underside of tail same color pattern as body, with both blotches and midventral streak terminating at tail tip. A single male specimen (QHU R2024049) is the only representative of the second morph (Fig. 15). In this specimen, the dorsal ground color is reddish brown. Paravertebral stripes dark brown, well-defined anteriorly, but fainter from midbody and onwards, blending with surrounding dorsal surface. Middorsal space between each stripe orange red. Head gold brown, all markings dark brown with no light pigment medially. Ventral surface of head is tan

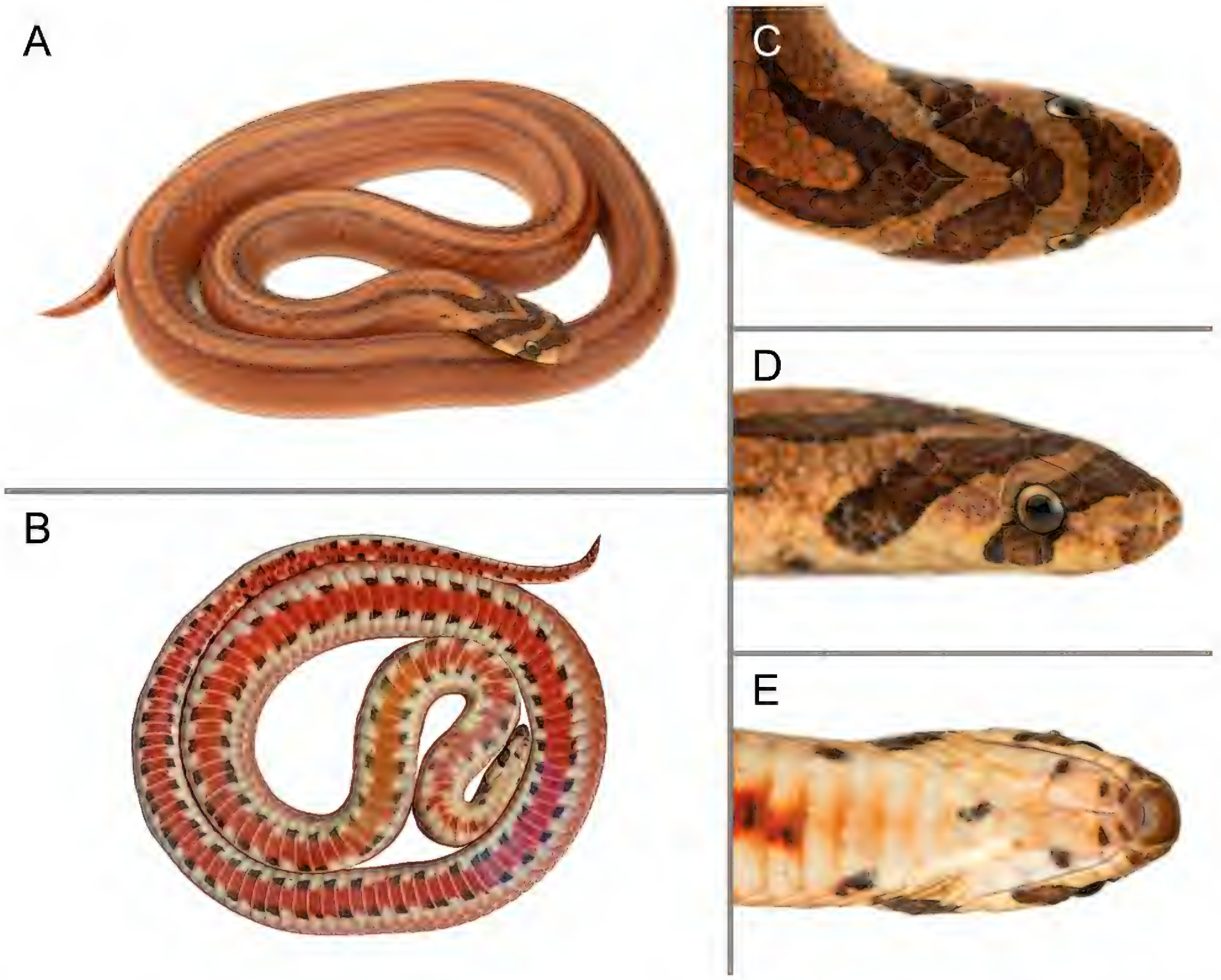

Figure 14. Coloration of the typical morph of *Oligodon bivirgatus* in life (uncollected adult male, iNaturalist 298113949). **A.** Dorsolateral view; **B.** Ventral view; **C.** Dorsal view of the head; **D.** Lateral view of the head; **E.** Ventral view of the head. Photographs by B.W. Genter.

Figure 15. Coloration of the new morph of *Oligodon bivirgatus* in life (QHU R2024049, adult male). Photographs by C.X. Liao and Y.H. Xu.

bearing a few scattered dark spots on each anterior chin shield and a single spot on the median gular scales. Ventral surface orange red, pale spots present on lateral edges of the ventral scales anteriorly, sparser by midbody. Remaining underside of body and tail immaculate.

Coloration in preservative. In preservative after four years, ground color of typical morph brown dorsally, paravertebral stripes dark brown (Fig. 16A, B). Ventral surface white. Orange red midventral streak no longer visible, but rectangular blotches remain distinct. Second morph pale reddish brown after more than 12 months of preservation (Fig. 16C). The previously indistinct narrow dark stripes are more clearly visible. Ventral surface uniformly pale yellow, light blotches absent or faded.

Description of hemipenis (Fig. 17). Based on everted left organ of one adult male (QHU R2024049). Upon full eversion, total length of hemipenis 13.12 mm, width 3.23 mm. Hemipenis thin, short, cylindrical, and unilobed, with a nearly circular cross-section, extending to the 7th subcaudal scale when fully everted. Both sulcate and asulcate surfaces densely covered with spinous calyces, basal hooks absent. The proximal quarter with smaller and sparse spinules gradually transitioning into larger, more evenly distributed keratinized spines distally, including apical surface. *Sulcus spermaticus* simple, undivided, extending centripetally from lateral portion of base to median apex. Sulcus lips well-developed and raised, their walls smooth.

Distribution and natural history. Endemic to Hainan Island, China, where it is confirmed from three localities in the southern portion of the island: Shangxi Nature Reserve, Jianfengling National Forest Park, and Diaoluo Mountain (Diaoluoshan) (Fig. 1, Suppl. material 1: table S1). All known sites are situated at low-to-mid elevations of (319–1,042 m asl.) and are characterized by montane and bamboo forests. A previous record of *Oligodon ornatus* from Jianfengling National Forest Park may also refer to this species (Kadoorie Farm and Botanic Garden 2001). The male specimen from Diaoluoshan Mountain (QHU R2024049) was observed active in broadleaf forest during the afternoon (Fig. 18). Another male specimen from Jianfengling (iNaturalist 298113949) was encountered alive on forested slope adjacent to paved road approximately 1–2 hours after sunset, while an additional individual from the same area (SYS r002952) was found dead on the road.

Conservation status. Currently, *Oligodon bivirgatus* is known only from three independent localities in Hainan Province, China. Based on GeoCAT analyses, the species has an EOO of 1,073.3 km^2 and an AOO of 546.9 km^2. Field surveys further indicate that the species is restricted to elevations between 319 and 1,042 m asl., occurring only in well-preserved primary broadleaf forests and adjacent bamboo forests. No individuals have been recorded from lower elevations where habitats are more heavily affected by human activities. As the species is known from fewer than five locations and its habitat is susceptible to disturbance, it meets the conditions of Vulnerable D2. We therefore recommend assessing *Oligodon bivirgatus* as Vulnerable (VU).

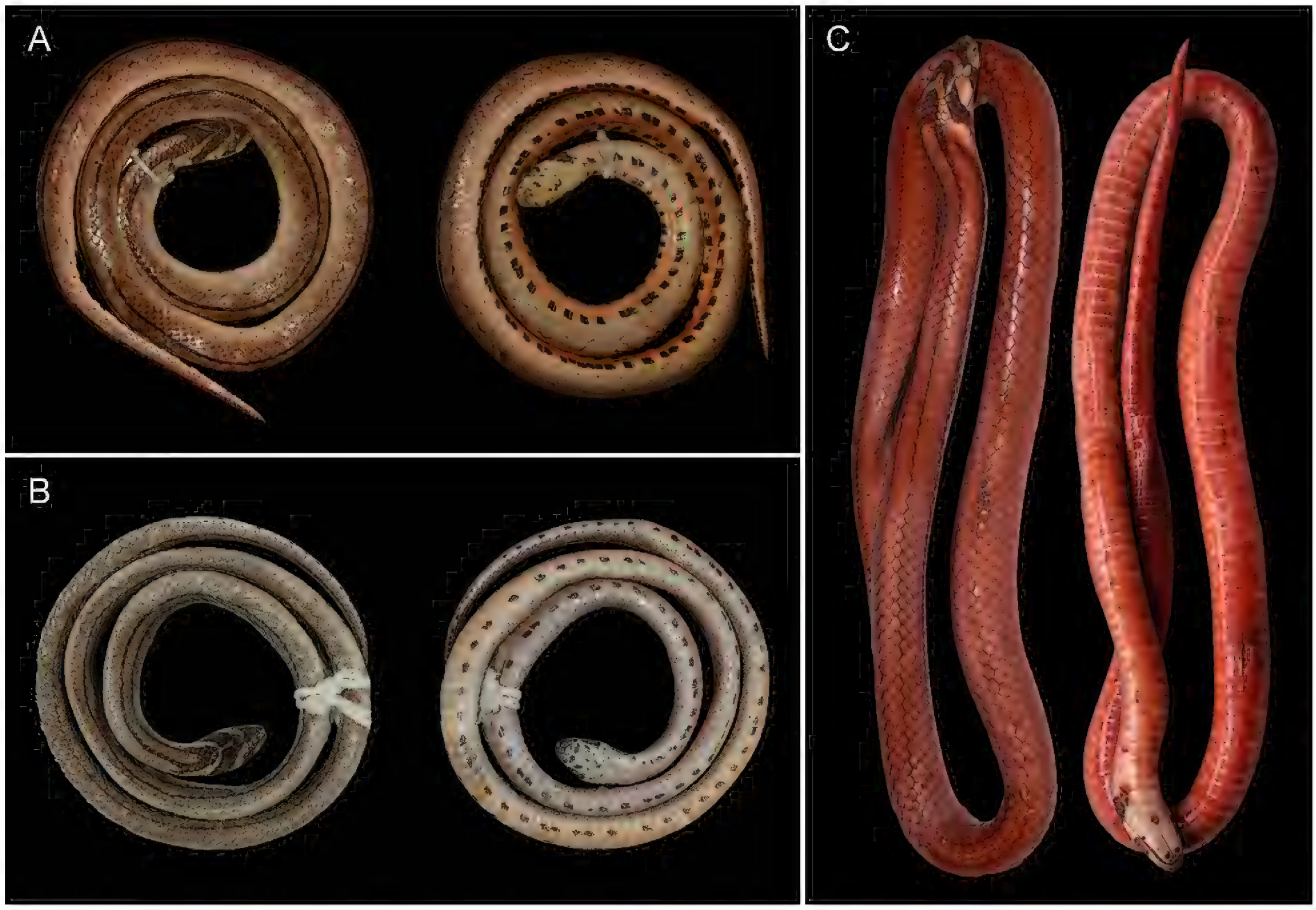

Figure 16. Preserved specimens of *Oligodon bivirgatus*. **A.** Holotype SYNU 1907027, adult female; **B.** Paratype SYNU 1808001, adult female; **C.** QHU R2024049, adult male representing the new color morph. Photographs reproduced from Qian et al. (2021) (**A, B**) and by Y.H. Xu (**C**)

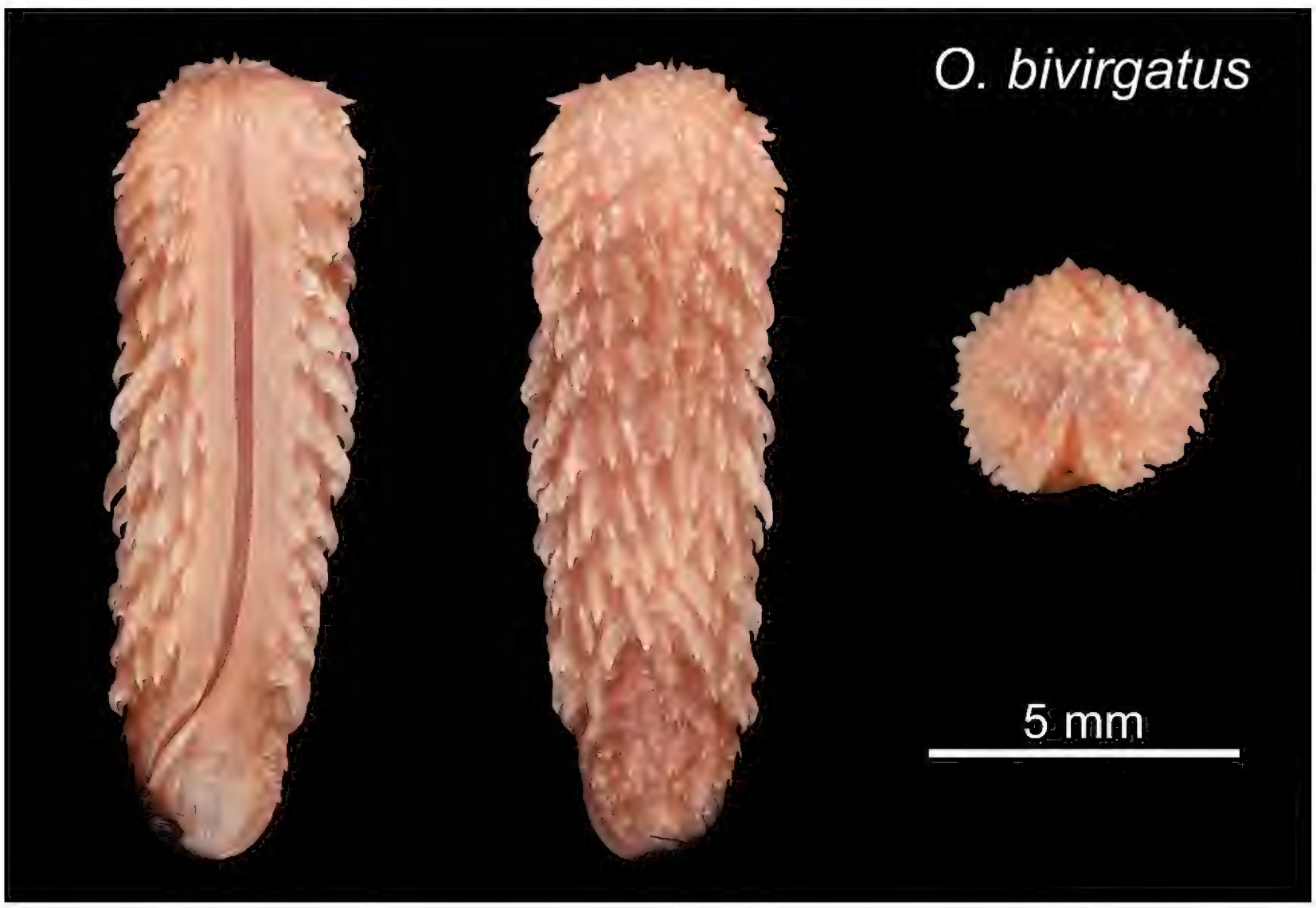

Figure 17. Sulcus side (left), asulcate side (middle), and apical side (right) of the hemipenis of *Oligodon bivirgatus* (QHU R2024049, adult male). Photographs by J.J. Huang and J.L. Ren. Scale bar: 5 mm.

Figure 18. Habitat of *Oligodon bivirgatus* in Diaoluoshan, Lingshui Li Autonomous County, Hainan Province, China. Photograph by C.X. Liao.

Discussion

By combining detailed morphological data with new phylogenetic evidence, we confirm that *O. ornatus*, *O. lungshenensis*, and *O. bivirgatus* should be recognized as valid species (Table 3). In terms of both color pattern and scalation, *O. ornatus* is undoubtedly most similar to *O. lungshenensis*, which has led to long-standing confusion and occasional misidentifications between the two (Zhao et al. 1986; Zhao and Yang 1997; Zhao 2002; Li et al. 2020). However, *O. ornatus* is reliably distinguished from *O. lungshenensis* by the presence of internasals (Figs 5, 9), a stable character absent in *O. lungshenensis*, as well as by the presence of keratinized spines covering the entire hemipenis except for the basal one-eighth and parts of the apical surface (vs. spines gradually decreasing in size past the midpoint of the organ, distal one-fifth, and the apical surface nude in *O. lungshenensis*, Figs 8, 12). *O. lungshenensis* also has a lower mean relative tail length, subcaudal scales and subcaudal ratio than *O. ornatus* (see *P*-values for characters in Table 3). However, the most informative of these three characters appears to be the difference in relative tail length in male specimens, which barely overlaps (TailLR 0.114–0.147 [$\overline{x}$ = 0.132 ± 0.012; N = 14] vs. 0.145–0.163 [$\overline{x}$ = 0.151 ± 0.007; N = 8] in *O. ornatus*). Male *O. ornatus* and *O. bivirgatus* (data after vs.) are differentiated by having more ventral scales (160–173 vs. 150–156) and a higher number of total body scales (199–217 vs. 184–193). The two species also possess completely different dorsal color patterns (dark brown dorsal bands in *O. ornatus* vs. narrow paravertebral stripes in *O. bivirgatus*). By contrast, the species that are phylogenetically more closely related, *O. lungshenensis* and *O. bivirgatus* (data after vs.) – exhibit more pronounced morphological differences. Compared to *O. bivirgatus*, *O. lungshenensis* lacks internasal scales (vs. present), has a higher ventral scale count in males (163–185 vs. 150–156), a higher number of total body scales in males (198–215 vs. 184–193), and a completely different dorsal color pattern (dorsal bands vs. paravertebral stripes, Figs 11, 16). Additionally, the spines on the hemipenis of *O. lungshenensis* gradually decrease in size from the middle toward the apex, and the distal one-fifth and apical surface are entirely nude (vs. uniformly sized spines covering the entire hemipenis in *O. bivirgatus*, Figs 12, 17).

All three focal *Oligodon* species (*O. bivirgatus*, *O. lungshenensis*, and *O. ornatus*) share a unique head scale configuration in which the lower anterior temporal is blocked from contacting the postocular and the lip, leading to narrow contact between the penultimate and ultimate supralabial. Following McDowell (1967), we have used the term 'temporolabial' throughout the text to identify this condition when it occurs (Fig. 19). The presence of the character normally results in a temporal formula of 2+2 in our sample, but rare fusions between scales on the upper and lower anterior row have been recorded in *O. ornatus* (Pope 1935; Zhao et al. 1998). This is the case in the holotype of *Simotes musyi* (Roux 1919; this study; Suppl. material 1: fig. S2) and UMMZ 182640. Although Qian et al. (2021: 408) recorded a temporal formula of 1+2 for *O. bivirgatus*, they stated the sixth supralabial was "excluded from the lip." Nonetheless, it is obvious that the type specimens of *O. bivirgatus* figured in their description have an identical scale configuration as *O. lungshenensis* and *O. ornatus*; there is a large diamond-shaped scale below the upper anterior temporal that does not contact the postocular or lip yet is "squeezed" between the two posteriormost supralabials (Fig. 13). We originally considered the presence of the temporolabial to be a putative autapomorphy of the

Table 3. Summary of morphological characters among *O. bivirgatus*, *O. lungshenensis*, and *O. ornatus*, based on examined material and literature data. Ranges for body scale counts and relative tail length are presented separately for male and female specimens. Sample sizes (N) for individual characters may vary (see species accounts for further details). All other scale and color pattern characters include combined male and female values. Refer to the Materials and methods for abbreviations of morphological characters. Bold text indicates interspecific diagnostic characters that can be used to distinguish among species.

Species	*O. bivirgatus*		*O. lungshenensis*		*O. ornatus*	
Sex	♂	♀	♂	♀	♂	♀
N	3	2	16	14	11	2
TailLR	0.136–0.164	0.121–0.131	0.114–0.147	0.106–0.133	0.145–0.163	0.119–0.128
VEN	**150–156**	173–176	**163–185**	167–186	**160–173**	171–185
SC	33–37	34–37	31–40	31–35	34–43	31–35
TOTAL	**184–193**	211	**198–215**	201–218	**199–217**	203–221
SCR	0.179–0.192	0.161–0.175	0.148–0.188	0.142–0.172	0.171–0.205	0.153–0.158
MT	8		8		7–8	
INS	**Present**		**Fused**		**Present**	
SL	6		6 (rarely 5)		6 (rarely 5)	
IL	6–7		6–7 (rarely 5)		6–7	
PreOc	1		1		1	
PostOc	2		1–2		2	
TEMP	2+2		2+2 (rarely 2+1)		2+2 (rarely 1+1, 2+1, 1+2)	
BBand	**Absent**		**7–11**		**8–10**	
TBand	**Absent**		**1–3**		**1–2**	
TotBand	**Absent**		**9–14**		**10–12**	

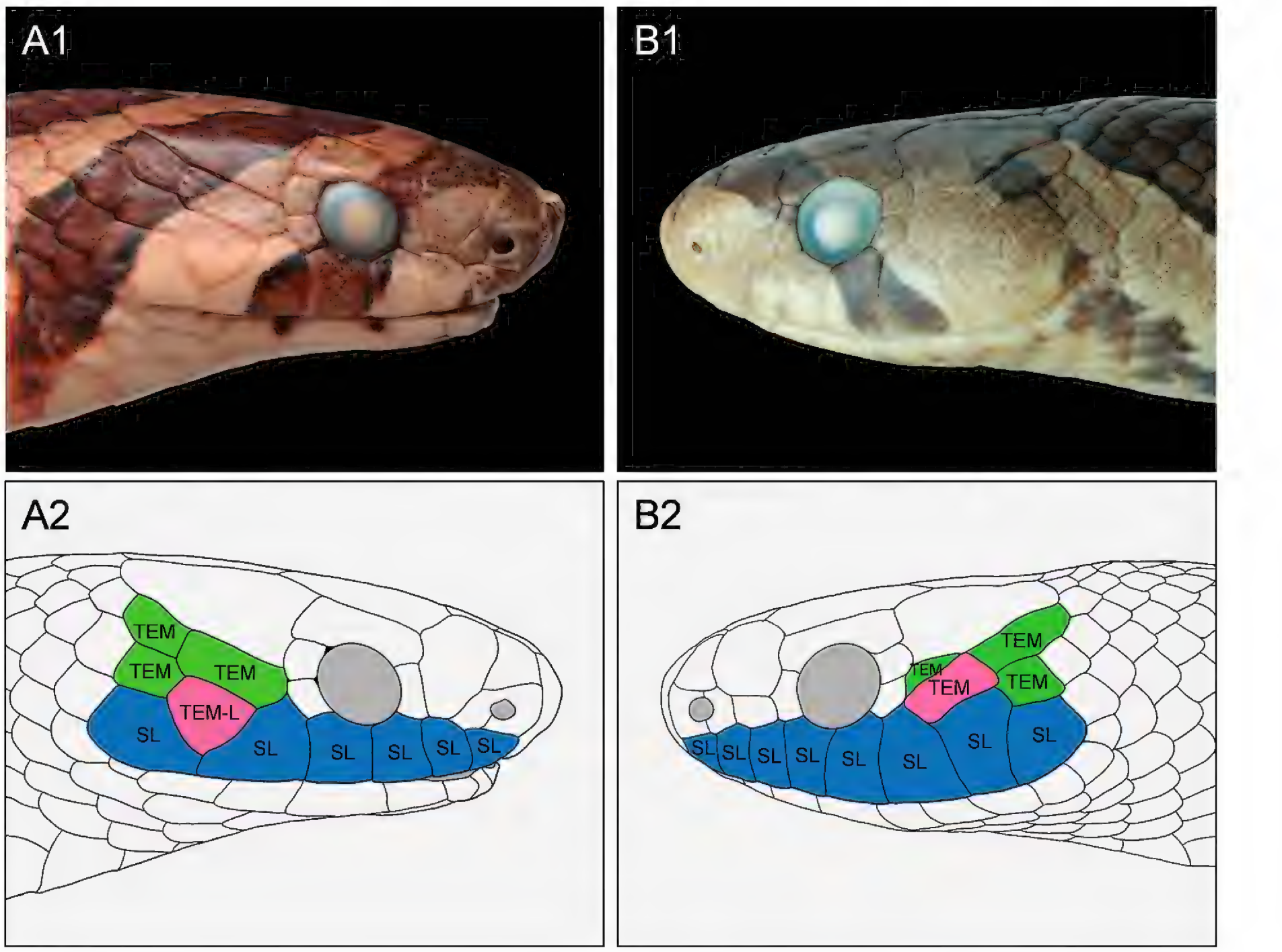

Figure 19. Photographs (**A1, B1**) and drawings (**A2, B2**) illustrating the specialized configuration of the lower anterior temporal scale (**A**, exemplified by *O. bivirgatus*; specimen QHU R2024049) in *Oligodon* and the non-specialized condition (**B**, exemplified by *O. chinensis* (Günther, 1888); specimen QHU R2023015). Notes: **SL**: supralabials; **TEM**: temporals; **TEM-L**: temporolabial. Photographs and drawings by Y.H. Xu.

O. bivirgatus, *O. lungshenensis*, and *O. ornatus* clade, but soon realized this was not the case after identifying at least six *Oligodon* species where descriptions consistently note the existence of the same supralabial-temporal scale configuration. These examples include *O. erythrogaster* Boulenger, 1907; *O. meyerinkii* (Steindachner, 1891); *O. nikhili* Whitaker & Dattatri, 1982; *O. octolineatus* (Schneider, 1801); *O. transcaspicus*; and *O. venustus* (Jerdon, 1853) (based on Günther 1864; Wall 1909; Taylor 1922; Tillack and Günther 2009; Lee et al. 2023; and original descriptions cited therein). Wall (1922, 1923) also identified four additional species where the penultimate supralabial was "cuneate… [and] fails to reach the upper lip" (Wall 1923: 316), namely *O. arnensis* sensu lato (Shaw, 1802); *O. calamarius* (= as *O. templetoni* Günther, 1862); *O. melanozonatus* Wall, 1922; and *O. taeniolatus* Jerdon, 1853; however, these examples were considered abnormalities from the typical scale conditions of each taxon. We did not observe any significant pattern associated with the temporolabial scale after mapping its presence/absence across genetically sampled *Oligodon* species in Lee et al. (2024), except that the trait likely evolved independently in multiple intrageneric groups. Aside from the observation that fossorial snake species tend to evolve fusions in head scale suturing (Resetar and Marx 1981; Savitzky 1983), the functional significance of the temporolabial in this genus is largely unclear.

What is clear is there are many ways that authors have attempted to score the lower anterior temporal condition across *Oligodon*, albeit none of them used the term "temporolabial" to describe this trait. Günther (1864) included the lower anterior temporal as part of the supralabial count in his description of *O. venustus* but noted when the scale was blocked from contacting the lip. This interpretation was followed in subsequent descriptions by Wall (1909, 1922, 1923), Whitaker and Dattatri (1982), and Qian et al. (2021). Other workers working with *Oligodon* simply included the temporolabial as part of the anterior temporal (Boulenger 1894, 1907; Taylor 1922; Zhao et al. 1998; Tillack and Günther 2009) or the posterior temporal count (Lee et al. 2023). These inconsistencies interpreting scale identities highlight a potential source of error in morphological comparisons and species diagnoses, so a standard approach to scoring the supralabials and temporal scales is desirable. The most prominent use of the term 'temporolabial' is in Australia and Melanesia, where a large number of elapid snakes present similar supralabial and temporal scale configurations (McDowell 1967; Shea et al. 1993; Greer 1997; Scanlon 2003; Scanlon and Lee 2004). The general counting system followed by authors is to consider the temporolabial as part of the anterior temporal row irrespective of whether it contacts the postocular scales or not. If, however, the temporolabial contacts the lip, it is included in the supralabial count (Shea 1998; Scanlon and Lee 2004). Here, we favor this approach to counting both scale characteristics, which is consistent with the way Zhao et al. (1998) counted supralabials and temporals in *O. lungshenensis* and *O. ornatus*, as did Boulenger (1894) and Taylor (1922). To avoid misidentifications and promote taxonomic clarity, we strongly recommend that future studies adopt this approach for scoring both supralabial and temporal scales in *Oligodon* or at least provide explanations as to how each character was scored. Finally, although the temporolabial scale is widespread across several Australian elapid genera, its presence within Colubridae is poorly documented. Aside from *Oligodon*, the only other colubrid genera in Asia with a similar temporal-supralabial configuration are *Plagiopholis* Boulenger, 1893, and *Sibynophis* Fitzinger, 1843 (Fitzinger 1843; Boulenger 1893; Pope 1935; Smith 1943; Captain et al. 2004; Cai et al. 2025; Nguyen and Vogel 2025; Qi et al. 2025b).

This study provides the first high-resolution images of the hemipenes of *Oligodon ornatus*, *O. lungshenensis*, and *O. bivirgatus*, along with detailed descriptions and comparisons. Our findings highlight the potential of hemipenial morphology as a valuable tool for species identification within *Oligodon*, provided that the organ is everted and interpreted consistently (Yushchenko et al. 2023a, b; Lee et al. 2025). In snakes, scalation and coloration are traditionally the most important morphological characters used for species recognition and taxonomic classification. However, in *Oligodon*, these characteristics can be highly conserved across species or highly labile, making species delimitation particularly challenging without a careful analysis of comparative material. For instance, *O. ornatus* and *O. lungshenensis* are nearly identical in all scalation traits, differing only in the presence (vs. absence) of internasals. In contrast, the hemipenes of *O. ornatus*, *O. lungshenensis*, and *O. bivirgatus* seem to exhibit clear and consistent differences in the size and distribution of spines and overall shape (Figs 8, 12, 17). These distinctions suggest that hemipenial morphology may provide important diagnostic characters for species-level taxonomy in *Oligodon*. That said, our sample size for these species is limited, and the extent to which *Oligodon* taxa exhibit intraspecific variation in hemipenial morphology remains poorly understood. We therefore recommend future studies place greater emphasis on examining and documenting hemipenial morphology across a broader range of *Oligodon* species. Such efforts will be critical for resolving the taxonomic complexity within this morphologically conservative and often confusing group.

Both branching patterns and dating analyses suggest *Oligodon bivirgatus*, *O. lungshenensis*, and *O. ornatus* diverged recently during the Pliocene and early Pleistocene. Lee et al. (2024) estimated the mean divergence of *O. ornatus* at approximately 4.4 Mya, followed by another split between *O. lungshenensis* and *O. bivirgatus* at 2.8 My. The presence of *O. bivirgatus* on Hainan Island relative to its phylogenetic position and estimated divergence time is of biogeographic interest. Evidence from geological and paleoclimatic studies suggests Hainan Island underwent repeated cycles of isolation and connection throughout the Cenozoic, but the exact timing and

tectonic history of these events remain controversial (Zhu 2016, 2025; Liang et al. 2018; Huo et al. 2022; Huang et al. 2024; Ali et al. 2025). Nonetheless, the split between *O. bivirgatus* and *O. lungshenensis* predates the isolation of Hainan from mainland Asia through the formation of the Qiongzhou Strait between 2.5–2.0 My, after which volcanism, sea level changes, and glacial cycles led to recurring stages of separation and re-connection between each landmass in the Quarternary (Zhao et al. 2007; Zhu 2016). We hypothesize that the ancestor of *O. bivirgatus* probably originated in present-day Guangdong Province and colonized Hainan via dispersal through the Leizhou Peninsula. This scenario is supported by similar biogeographic patterns in both endemic and non-endemic species of herpetofauna native to the island (Zhao 1990; Huang et al. 2013; Zhu et al. 2016; Yu et al. 2020; Qi et al. 2025a), most of which are of Plio-Pleistocene origin (Ali et al. 2025).

It is also interesting that the distributions of *Oligodon ornatus* and *O. lungshenensis* largely follow a longitudinal cline, with the former species inhabiting the Wuyi and Luoxiao mountains and the latter inhabiting the Nanling and Wuling mountains as well as the Yunnan-Guizhou plateau (Fig. 1). All five landscapes are recognized as important biodiversity hotspots, functioning as refugia during Quarternary glacial cycles and corridors facilitating dispersal and speciation in many floral and faunal groups (Liu et al. 2012; Gong and He 2008; Tian et al. 2018; Lyu et al. 2024). As a result, it is possible these landscapes facilitated cladogenesis between *O. ornatus* and *O. lungshenensis* through vicariance. Similar east-to-west patterns of lineage structure have been detected in other snakes that are dependent on montane forest biomes, including *Deinagkistrodon acutus* (Günther, 1888) (Huang et al. 2007) and several members of the genus *Opisthotropis* Günther, 1872 (Ren et al. 2025b). That said, the division between *O. ornatus* and *O. lungshenensis* is not perfect. Both species overlap in range at multiple localities in Hunan Province (Shen et al. 2014; Gao et al. 2022) and may be putatively sympatric at several localities in the Nanling mountains based on mitochondrial DNA and morphological data (Yuan et al. 2010; Wu et al. 2023). We say "putative" insofar as we assume that the observed matrilineal divergence between species is also reflected across the nuclear genome in areas of co-occurrence. Unfortunately, while we obtained nuclear DNA from *O. lungshenensis* throughout Hunan Province, we were not able to generate comparative nuclear data from *O. ornatus* occurring at the same localities. Mitochondrial introgression and incomplete lineage sorting could obscure gene flow or secondary contact between *O. lungshenensis* and *O. ornatus*, even if the two species are not necessarily their closest relatives (McGuire et al. 2007; Rabosky et al. 2009; Qi et al. 2014; Myers et al. 2024). However, given the primary morphological feature separating each species (the presence/absence of internasals) appears fixed in areas of putative sympatry, this conjecture, although possible, seems unlikely.

Acknowledgments

We thank Song Huang (ANU, China), Jianping Jiang (CIB, China), Denis Vallan and Raffael Winkler (NHMB, Switzerland), Yingyong Wang and Hanming Song (SYS, China), Gregory E. Schneider and Daniel Rabosky (UMMZ, USA), and Valentina Orlova (ZMMU, Russia) for permission to examine specimens under their care. We sincerely thank Jinlong Ren and Junjie Huang (CIB, China) for their invaluable assistance with the preparation, photography, and morphological description of the hemipenes of *Oligodon bivirgatus*. We thank Yang Ge (Hainan, China) for his assistance with fieldwork. We thank Binqing Zhu (China) for providing photographs of *O. ornatus*. BWG would like to thank Kevin Messenger (Nanjing Forest University, China) for supporting his fieldwork, which led to the observation of another *O. bivirgatus* specimen. We also thank Tan Van Nguyen (Duy Tan University, Vietnam) and Song Huang (ANU) for constructive comments on the manuscript. All sampling procedures involving live snakes were in accordance with the Wild Animal Protection Law of China and approved by the Institutional Ethics Committee of Qinghai University (protocol code PJ202501-89). This research was funded by the Qinghai Science & Technology Department [2024-ZJ-965], the National Natural Science Foundation of China [32301325], and the Russian Science Foundation (RSF grant N° 22-14-00037-P, for supporting the work of Dr. Nikolay A. Poyarkov).

References

Ali JR, Li Y-X, Fritz U (2025) Biogeography of Hainan Island, southern China, and the falsification of the 'shifting-landmass' hypothesis. Palaeogeography, Palaeoclimatology, Palaeoecology 666: e112832. https://doi.org/10.1016/j.palaeo.2025.112832

Bouckaert R, Heled J, Kühnert D, Vaughan T, Wu CH, Xie D, Suchard MA, Rambaut A, Drummond AJ (2014) BEAST 2: A software platform for Bayesian evolutionary analysis. PLoS Computational Biology 10: e1003537. https://doi.org/10.1371/journal.pcbi.1003537

Boulenger GA (1893) Catalogue of the snakes in the British Museum (Natural History) (Vol. I). Containing the families Typhlopidæ, Glauconiidæ, Boidæ, Ilysiidæ, Uropeltidæ, Xenopeltidæ, and Colubridæ Aglyphæ, part. Order of the Trustees, British Museum (Natural History), London, xiii + 448 pp. [28 pls.] https://doi.org/10.5962/bhl.title.8316

Boulenger GA (1894) Catalogue of the snakes in the British Museum (Natural History) (Vol. II). Containing the conclusion of the Colubridæ Aglyphae. British Museum (Natural History), London, xi + 382 pp.

Boulenger GA (1907) Description of a new snake from Nepal. Records of the Zoological Survey of India 1(3): e217. https://doi.org/10.26515/rzsi/v1/i3/1907/163394

Burbrink FT, Lawson R, Slowinski JB (2000) Mitochondrial DNA phylogeography of the polytypic North American rat snake (*Elaphe obsoleta*): A critique of the subspecies concept. Evolution; International Journal of Organic Evolution 54: 2107–2118. https://doi.org/10.1554/0014-3820(2000)054[2107:MDPOTP]2.0.CO;2

Cai B, Xu Y, Vogel G, Peng L, Xu J, Cheng L, Liang D, Li M, Wang Y, Ma S (2025) Redescription of *Plagiopholis styani* (Serpentes, Pseudoxenodontidae), with description of two new species from China. Zoosystematics and Evolution 101(4): 1775–1797. https://doi.org/10.3897/zse.101.152739

Captain A, Gower D, David P, Bauer AM (2004) Taxonomic status of the colubrid snake *Sibynophis subpunctatus* (Duméril, Bibron & Duméril, 1854). Hamadryad 28(1–2): 90–94.

Che J, Chen H-M, Yang J-X, Jin J-Q, Jiang K, Yuan Z-Y, Murphy RW, Zhang Y-P (2012) Universal COI primers for DNA barcoding amphibians. Molecular Ecology Resources 12(2): 247–258. https://doi.org/10.1111/j.1755-0998.2011.03090.x

Chen BH (1991) The Amphibian and Reptilian Fauna of Anhui. Anhui Science and Technology Publishing House, Hefei, 408 pp. [in Chinese]

Chiari Y, Vences M, Vieites DR, Rabemananjara F, Bora P, Ramilijaona, Ravoahangimalala O, Meyer A (2004) New evidence for parallel evolution of colour patterns in Malagasy poison frogs (*Mantella*). Molecular Ecology 13: 3763–3774. https://doi.org/10.1111/j.1365-294X.2004.02367.x

Darko YA, Voss O, Uetz P (2022) A dictionary of abbreviations used in reptile descriptions. Zootaxa 5219(5): 421–432. https://doi.org/10.11646/zootaxa.5219.5.2

De Queiroz K (2007) Species concepts and species delimitation. Systematic Biology 56(6): 879–886. https://doi.org/10.1080/10635150701701083

Dong J, Deng ZS, Yang CX, Wang JL (2023) A new record species of snake in Hubei Province, *Oligodon lungshenensis*. Sichuan Journal of Zoology 42(2): 197–198. [in Chinese]

Dowling HG (1951) A proposed standard system of counting ventrals in snakes. British Journal of Herpetology 1: 97–99.

Dowling HG, Savage JM (1960) A guide to the snake hemipenis: A survey of basic structure and systematic characteristics. Zoologica 45(2): 17–28. https://doi.org/10.5962/p.203350

Fitzinger L (1826) Neue Classification der Reptilien nach ihren natürlichen verwandtschaften: Nebst einer Verwandtschaftstafel und einem Verzeichnisse der Reptilien-sammlung des K. K. zoologischen Museum's zu Wien. J. G. Heubner, Wien, [12] + 61 pp. [+ [11] + 1 foldout pl.] https://doi.org/10.5962/bhl.title.4683

Fitzinger L (1843) Systema Reptilium. Fasciculus Primus. Braumüller et Seidel, Vindobonae, 106 [+ vi + [3]] pp. https://doi.org/10.5962/bhl.title.4694

Gao Z, Qian T, Jiang J, Hou D, Deng X, Yang D (2022) Species diversity and distribution of amphibians and reptiles in Hunan Province, China. Shengwu Duoyangxing 30: e21290. https://doi.org/10.17520/biods.2021290

Gong W, Liu W, Gu L, Kaneko S, Koch MA, Zhang D (2016) From glacial refugia to wide distribution range: demographic expansion of *Loropetalum chinense* (Hamamelidaceae) in Chinese subtropical evergreen broadleaved forest. Organisms Diversity & Evolution 16: 23–38. https://doi.org/10.1007/s13127-015-0252-4

Gong S, He B (2008) A new record of *Oligodon ornatus* in Guangdong Province. Sichuan Journal of Zoology 21(2): e239. [in Chinese]

Greer AE (1997) The Biology and Evolution of Australian Snakes. Surrey Beatty & Sons, Chipping Norton, New South Wales, 358 pp.

Günther ACLG (1862) On new species of snakes in the collection of the British Museum. Annals and Magazine of Natural History; Zoology, Botany, and Geology, Series 3 9(49): 52–59. [+ pls. 9–10.] https://doi.org/10.1080/00222936208681186

Günther ACLG (1864) The reptiles of British India. R. Hardwicke [The Ray Society], London, xxvii + 452 pp. [+ 26 pls.] https://doi.org/10.5962/bhl.title.5012

Günther ACLG (1888) On a collection of reptiles from China. Annals and Magazine of Natural History; Zoology, Botany, and Geology, Series 4 6(3): 165–172. [+ pl. 12.] https://doi.org/10.1080/00222938809460702

Hedges SB (1994) Molecular evidence for the origin of birds. Proceedings of the National Academy of Sciences of the United States of America 91: 2621–2624. https://doi.org/10.1073/pnas.91.7.2621

Huang M (1990) Fauna of Zhejiang: Amphibia, Reptilia. Zhejiang Science and Technology Publishing House, Hangzhou, 306 pp. [in Chinese].

Huang S (2023) Sinoophis: Atlas of snakes in China (Vols. 1 & 2). The Straits Publishing & Distribution Group, Fuzhou, 284 pp. [+ 645 pp.] [in Chinese]

Huang Z-J, Zheng J, Fang J-J (1978) New species of snakes. Journal of Fujian Normal University, Natural Science series 1978(2): 91–93. [in Chinese]

Huang S, He S, Peng Z, Zhao K, Zhao E (2007) Molecular phylogeography of endangered sharp-snouted pitviper (*Deinagkistrodon acutus*; Reptilia, Viperidae) in mainland China. Molecular Phylogenetics and Evolution 44(3): 942–952. https://doi.org/10.1016/j.ympev.2007.05.019

Huang Y, Guo X, Ho SYW, Shi H, Li J, Li J, Cai B, Wang Y (2013) Diversification and demography of the oriental garden lizard (*Calotes versicolor*) on Hainan Island and the adjacent mainland. PLoS ONE 8(6): e64754. https://doi.org/10.1371/journal.pone.0064754

Huang P-H, Wang T-R, Li M, Lu Z-J, Su R-P, Fang O-Y, Li L, Zhou S-S, Tan Y-H, Meng H-H, Song Y-G, Li J (2024) RAD-seq data for *Engelhardia roxburghiana* provide insights into the palaeogeography of Hainan Island and its relationship to mainland China since the late Eocene. Palaeogeography, Palaeoclimatology, Palaeoecology 651: e112392. https://doi.org/10.1016/j.palaeo.2024.112392

Huo X, Yang Z, Xie Y, Yang Y (2022) Tempo and mode of floristic exchanges between Hainan Island and mainland Asia: A case study of the *Persea* group (Lauraceae). Forests 13(10): e1722. https://doi.org/10.3390/f13101722

IUCN (2012) IUCN Red List categories and criteria, version 3.1, (2nd edn.). IUCN, Gland, Switzerland.

Jerdon TC (1853) Catalogue of reptiles inhabiting the peninsula of India. Journal of the Asiatic Society of Bengal 22(6): 522–534.

Jiang K (2010) A method for evaginating the hemipenis of preserved snakes. Sichuan Journal of Zoology 29: 122–123. [in Chinese]

Jiang K, Wu DH, Huang JJ, Ren JL, Gao ZY, Lyu ZT, Li JT (2025) Description of a new species of kukri snake (Serpentes: Colubridae: *Oligodon*) from Xizang, China. Asian Herpetological Research 16(1): 36–48. [registered online in 2024] https://doi.org/10.3724/ahr.2095-0357.2024.0058

Kadoorie Farm and Botanic Garden (2001) Report of rapid biodiversity assessments at Jianfengling Nature Reserve, Southwest Hainan, 1998 and 2001. South China Forest Biodiversity Survey Report Series (online simplified version), no. 3. Kadoorie Farm and Botanic Garden, Hong Kong, ii + 35 pp.

Kaiser CM, O'Shea M, Kaiser H (2019) A new species of Indo-Papuan groundsnake, genus *Stegonotus* Duméril et al., 1854 (Serpentes, Colubridae), from the Bird's Head Peninsula of West Papua, Indonesia, with comments on differentiating morphological characters. Zootaxa 4590(2): 201–230. https://doi.org/10.11646/zootaxa.4590.2.1

Kalyaanamoorthy S, Minh BQ, Wong TKF, von Haeseler A, Jermiin LS (2017) ModelFinder: Fast model selection for accurate phylogenetic estimates. Nature Methods 14(6): 587–589. https://doi.org/10.1038/nmeth.4285

Katoh K, Standley DM (2013) MAFFT multiple sequence alignment software version 7: Improvements in performance and usability. Molecular Biology and Evolution 30: 772–780. https://doi.org/10.1093/molbev/mst010

Kuntz RE (1963) Snakes of Taiwan. Quarterly Journal of the Taiwan Museum 16: 1–79.

Lawson R, Slowinski JB, Crother BI, Burbrink FT (2005) Phylogeny of the Colubroidea (Serpentes): New evidence from mitochondrial and nuclear genes. Molecular Phylogenetics and Evolution 37: 581–601. https://doi.org/10.1016/j.ympev.2005.07.016

Lee TH (2005) Ecological patterns of distribution on gradients of elevation and species diversity of snakes in southern Taiwan. Amphibia-Reptilia 26(3): 325–332. https://doi.org/10.1163/156853805774408522

Lee JL, Yushchenko PV, Milto KD, Rajabizadeh M, Rastegar-Pouyani E, Jablonski D, Masroor R, Karunarathna S, Mallik AK, Dsouza P, Orlov N, Nazarov R, Poyarkov NA (2023) Kukri snakes *Oligodon* Fitzinger, 1826 of the western Palearctic with the resurrection of *Contia transcaspica* Nikolsky, 1902 (Reptilia, Squamata, Colubridae). PeerJ 11: e15185. https://doi.org/10.7717/peerj.15185

Lee JL, Yushchenko PV, Suwannapoom C, Pawangkhanant P, Grismer LL, Van Nguyen T, Deepak V, Narayanan S, Das S, Neang T, Lalremsanga HT, Yang JH, Jablonski D, Erkaya M, Vogel G, Bauer AM, Poyarkov NA (2024) A multi-gene phylogeny of the Asian kukri snakes (*Oligodon* Fitzinger, 1826): Sharpening the blade of the second largest serpent radiation (Reptilia, Squamata, Colubridae). Molecular Phylogenetics and Evolution 201: e108215. https://doi.org/10.1016/j.ympev.2024.108215

Lee JL, Yushchenko PV, Pal S, Deepak V, Vogel G, Poyarkov NA, Bauer AM, Lalremsanga HT (2025) Color polymorphism, taxonomic confusion and cryptic diversity in the kukri snake *Oligodon albocinctus* (Cantor, 1839) (Squamata, Colubridae). Zootaxa 5714: 1–69. https://doi.org/10.11646/zootaxa.5714.1.1

Li D (1989) A survey of reptiles in Leigongshan area. In: Matsui M, Hikida T, Goric RC (Eds) Current Herpetology in East Asia. Proceedings of the Second Japan-China Herpetological Symposium Kyoto, July 1988. Herpetological Society of Japan, Kyoto, i–ix + 521 pp.

Li JN, Liang D, Wang YY, Guo P, Huang S, Zhang P (2020) A large-scale systematic framework of Chinese snakes based on a unified multilocus marker system. Molecular Phylogenetics and Evolution 148: e106807. https://doi.org/10.1016/j.ympev.2020.106807

Liang B, Zhou R-B, Liu Y-L, Chen B, Grismer LL, Wang N (2018) Renewed classification within *Goniurosaurus* (Squamata, Eublepharidae) uncovers the dual roles of a continental island (Hainan) in species evolution. Molecular Phylogenetics and Evolution 127: 646–654. https://doi.org/10.1016/j.ympev.2018.06.011

Linnaeus C (1758) Systema Naturæ per Regna Tria Naturæ, Secundum Classes, Ordines, Genera, Species, cum Characteribus, Differentiis, Synonymis, Locis. Tomus I. Editio decima, reformata. Cum Privilegio S:ae R:ae M:tis Sveciae. Impensis Direct. Laurentii Salvii, Holmiae, vii + 819 + i pp. https://doi.org/10.5962/bhl.title.542

Liu J-Q, Sun Y-S, Ge X-J, Gao L-M, Qiu Y-X (2012) Phylogeographic studies of plants in China: Advances in the past and directions in the future. Journal of Systematics and Evolution 50(4): 267–275. https://doi.org/10.1111/j.1759-6831.2012.00214.x

Liu F, Liu Y, Liu Q, Guo P, Wu YY (2025) *Oligodon lungshenensis* found in Luzhou, Sichuan, China. Dongwuxue Zazhi 60(4): 613–618. [in Chinese]

Luo Y, Luo J, Gao H, Liu Y, Luo T, Luo Z, Hu X (2010) New record of snakes in Chongqing – Longsheng small-headed snake (*Oligodon lungshenensis*). Chinese Journal of Zoology 4: 38 + 101. [in Chinese]

Lyu B, Liu Q, Wu Y, Nguyen TQ, Che J, Nguyen SN, Myers EA, Burbrink FT, Guo P, Wang J (2024) Genomic analysis reveals deep population divergence in the water snake *Trimerodytes percarinatus* (Serpentes, Natricidae). Ecology and Evolution 14(4): e11278. https://doi.org/10.1002/ece3.11278

Maes D, Isaac NJ, Harrower CA, Collen B, Van Strien AJ, Roy DB (2015) The use of opportunistic data for IUCN Red List assessments. Biological Journal of the Linnean Society. Linnean Society of London 115: 690–706. https://doi.org/10.1111/bij.12530

Maki M (1931) Monograph of the Snakes of Japan. Dai-ichi Shobo, Tokyo, 240 pp. [in Japanese]

McDowell SB (1967) *Aspidomorphus*, a genus of New Guinea snakes of the Family Elapidae, with notes on related genera. Journal of Zoology 151(4): 497–543. https://doi.org/10.1111/j.1469-7998.1967.tb02130.x

McGuire JA, Linkem CW, Koo MS, Hutchison DW, Lappin AK, Orange DI, Lemos-Espinal J, Riddle BR, Jaeger JR (2007) Mitochondrial introgression and incomplete lineage sorting through space and time: Phylogenetics of Crotaphytid lizards. Evolution; International Journal of Organic Evolution 61(12): 2879–2897. https://doi.org/10.1111/j.1558-5646.2007.00239.x

Mell R (1931) List of Chinese snakes. Lingnan Science Journal 8(1929): 119–219.

Minh BQ, Schmidt HA, Chernomor O, Schrempf D, Woodhams MD, von Haeseler A, Lanfear R (2020) IQ-TREE 2: New models and efficient methods for phylogenetic inference in the genomic era. Molecular Biology and Evolution 37: 1530–1534. https://doi.org/10.1093/molbev/msaa015

Mori A, Narumi N, Kardong KV (1992) Unusual putative defensive behavior in *Oligodon formosanus* (Serpentes, Colubridae): Head-slashing and tail-striking. Journal of Herpetology 26(2): 213–216. https://doi.org/10.2307/1564865

Myers CW, Cadle JE (2003) On the snake hemipenis, with notes on *Psomophis* and techniques of eversion: A response to Dowling. Herpetological Review 34(4): 295–302.

Myers EA, Rautsaw RM, Borja M, Jones J, Grünwald CI, Holding ML, Grazziotin FG, Parkinson CL (2024) Phylogenomic discordance is driven by wide-spread introgression and incomplete lineage sorting during rapid species diversification within rattlesnakes (Viperidae, *Crotalus* and *Sistrurus*). Systematic Biology 73(4): 722–741. https://doi.org/10.1093/sysbio/syae018

Nguyen TV, Vogel G (2025) On the taxonomy of *Sibynophis grahami* (Boulenger, 1904) with remarks on morphology, distribution, natural history, and conservation status (Squamata, Sibynophiidae, *Sibynophis*). Zootaxa 5618(4): 525–551. https://doi.org/10.11646/zootaxa.5618.4.4

Nikolsky AM (1902) Gady i ryby [Herpetiles and Fishes]. Brockhaus-Efron, St. Petersburg, 872 pp. [in Russian and Latin]

Noonan BP, Chippindale PT (2006) Dispersal and vicariance: The complex evolutionary history of boid snakes. Molecular Phylogenetics and Evolution 40: 347–358. https://doi.org/10.1016/j.ympev.2006.03.010

Orlov NL, Ryabov SA, Nguyen T, Nguyen T (2010) Rediscovery and redescription of two rare snake species: *Oligodon lacroixi* Angel et Bourret, 1933 and *Maculophis bellus chapaensis* (Bourret, 1934) [Squamata: Ophidia: Colubridae] from Fansipan Mountains, northern Vietnam. Russian Journal of Herpetology 17(4): 310–322.

Oshima M (1910) An annotated list of Formosan snakes, with descriptions of four new species and one new subspecies. Annotationes Zoologicae Japonenses 7(3): 185–207. [in Japanese]

Palumbi S, Martin A, Romano S, McMillan WO, Stice L, Grabowski G (1991) The Simple Fool's Guide to PCR. Department of Zoology and Kewalo Marine Laboratory, University of Hawaii, Honolulu, 45 pp.

Paradis E, Schliep K (2019) ape 5.0: an environment for modern phylogenetics and evolutionary analyses in R. Bioinformatics 35(3): 526–528. https://doi.org/10.1093/bioinformatics/bty633

Patel H, Bhardwaj VK, Thackeray T, Campbell PD, Mirza ZA (2025) Phylogeny and systematics of *Oligodon juglandifer* (Wall, 1909) with comments on the taxonomic status of *Oligodon lipipengi* Jiang, Wang, Li, Ding, Ding & Che in Che et al. 2020. Diversity 17(3): e143. https://doi.org/10.3390/d17030143

Pauwels OSG, Donbundit N, Sumontha M, Meesook W (2025) *Oligodon cicadophagus*, a new kukri snake from southern peninsular Thailand (Squamata, Colubridae). Zootaxa 5569(2): 345–364. https://doi.org/10.11646/zootaxa.5569.2.7

Pope CH (1929) Notes on reptiles from Fukien and other Chinese provinces. Bulletin of the American Museum of Natural History 58(8): 335–487. [+ pls. 16–19.]

Pope CH (1935) The reptiles of China: turtles, crocodilians, snakes, lizards. Natural History of Central Asia 10. American Museum of Natural History, New York, lii + 604 pp. https://doi.org/10.5962/bhl.title.12104

Qi Y, Lu B, Gao H, Hu P, Fu J (2014) Hybridization and mitochondrial genome introgression between *Rana chensinensis* and *R. kukunoris*. Molecular Ecology 23(22): 5575–5588. https://doi.org/10.1111/mec.12960

Qi S, Ngo HN, Grismer LL, Wang HT, Song HM, Zhu XY, He ZQ, Zhou ZC, Li PP, Wang JC, Wang Y-Y (2025a) Integrative taxonomic revision of the *Goniurosaurus lichtenfelderi* group (Squamata: Eublepharidae): Insights from morphological and molecular data. Vertebrate Zoology 75: 673–698. https://doi.org/10.3897/vz.75.e158031

Qi S, Song HM, Yang HC, Xu YH, Fang RJ, Su JR, Liu ZF, Gong YN, Li FH, Lyu CH, Wang BY, Wang YY (2025b) A new species of *Plagiopholis* Boulenger, 1893 (Serpentes, Pseudoxenodontidae) from Guangdong, China. Zoosystematics and Evolution 101(4): 2171–2180. https://doi.org/10.3897/zse.101.172706

Qian TY, Qi S, Shi JS, Lu YY, Jenkins RWG, Mo YN, Li P (2021) A new species of *Oligodon* H. Boie in Fitzinger, 1826 (Squamata: Colubridae) from Hainan Island, China. Zootaxa 4933(3): 403–421. https://doi.org/10.11646/zootaxa.4933.3.7

R Core Team (2025) R: The R Project for Statistical Computing. Vienna. https://www.rproject.org [Last accessed 1 November 2025]

Rabosky DL, Talaba AL, Donnellan SC, Lovette IJ (2009) Molecular evidence for hybridization between two Australian desert skinks, *Ctenotus leonhardii* and *Ctenotus quattuordecimlineatus* (Scincidae, Squamata). Molecular Phylogenetics and Evolution 53(2): 368–377. https://doi.org/10.1016/j.ympev.2009.06.020

Rambaut A, Drummond AJ, Xie D, Baele G, Suchard MA (2018) Posterior summarization in Bayesian phylogenetics using Tracer 1.7. Systematic Biology 67(5): 901–904. https://doi.org/10.1093/sysbio/syy032

Ran H, Jie M, Zhen Y, Lei Z (2012) A new record of snake in Fodingshan Mountain Nature Reserve of Guizhou Province. Anhui Nongye Kexue 40(1): 199–200. [in Chinese]

Rao DQ, Zhou Z, Li P, Wang Y, Ding L (2024) *Oligodon ornatus*. The IUCN Red List of Threatened Species 2024: e. T192248A199544010. https://doi.org/10.2305/IUCN.UK.2024-1.RLTS.T192248A199544010.en [Accessed on 11 January 2026]

Ren JL, Jiang K, Huang JJ, David P, Li JT (2022) Taxonomic review of the genus *Herpetoreas* (Serpentes: Natricidae), with the description of a new species from Tibet, China. Diversity 14(2): 1–79. https://doi.org/10.3390/d14020079

Ren JL, Huang JJ, Wu W, Jiang K, Li JT (2025a) One mountain, two tigers: A new species of *Gloydius* (Serpentes, Viperidae) from the Upper Lancang Valley in Xizang, China, with comments on the diagnostic characters and evolution of the *G. strauchi* (Bedriaga, 1912) species complex. Asian Herpetological Research 16(1): 1–19. https://doi.org/10.3724/ahr.2095-0357.2024.0059

Ren JL, Li RH, Jia RW, Lyu ZT, Yan C, Jiang D, Wang YY, Li JT (2025b) Quaternary glaciation accelerates speciation in aquatic snakes through recent bottlenecks. Molecular Ecology 34(22): e70071. https://doi.org/10.1111/mec.70071

Resetar AR, Marx H (1981) A redescription and generic reallocation of the African colubrid snake *Elapocalamus gracilis* Boulenger with a discussion of the union of the brille and postocular shield. Journal of Herpetology 15(1): 83–89. https://doi.org/10.2307/1563650

Roux J (1919) Sur un nouveau serpent (*Simotes musyi*) provenant de la Chine. Revue Suisse de Zoologie, Genève 27(3): 61–63. https://doi.org/10.5962/bhl.part.36323

Savitzky AH (1983) Coadapted character complexes among snakes: Fossoriality, piscivory, and durophagy. American Zoologist 23(2): 397–409. https://doi.org/10.1093/icb/23.2.397

Scanlon JD (2003) The Australian elapid genus *Cacophis*: Morphology and phylogeny of rainforest crowned snakes. The Herpetological Journal 13: 1–20.

Scanlon JD, Lee MSY (2004) Phylogeny of Australasian venomous snakes (Colubroidea, Elapidae, Hydrophiinae) based on phenotypic and molecular evidence. Zoologica Scripta 33(4): 335–366. https://doi.org/10.1111/j.0300-3256.2004.00151.x

Schneider JG (1801) Historiae Amphibiorum Naturalis et Literariae. Fasciculus Secundus, Continens Crocodilos, Scincos, Chamaesauras, Boas, Pseudoboas, Elapes, Angues, Amphisbaenas et Caecilias. Friederici Frommann, Jenae, vi + 364 pp. [+ 2 pls.]

Shaw G (1802) General zoology, or systematic natural history (Vol. 3). Part II. Amphibia. G. Kearsley, London, vii + [2] + 303 pp.

Shea GM (1998) Geographic variation in scalation and size of the black whip snakes (Squamata: Elapidae: *Demansia Vestigiata* Complex): evidence for two broadly sympatric species. The Beagle. Records of the Museums and Art Galleries of the Northern Territory 14: 41–61. https://doi.org/10.5962/p.287491

Shea G, Shine R, Covacevich JC (1993) Family Elapidae. In: Glasby CG, Ross GJB, Beesley PL (Eds) Fauna of Australia (Vol. 2A), Amphibia and Reptilia. Australian Government Publishing Service, Canberra, 38 pp.

Shen YH, Ye YY, Deng XJ (2014) Fauna Hunan: Reptilia. Hunan Science and Technology Press, Changsha, 220 pp. [in Chinese]

Shi P, Zheng W (1985) Studies on feeding habits of the snakes of Mount Wuyi. Acta Herpetologica Sinica 4(2): 149–152. [in Chinese]

Smith MA (1943) The fauna of British India, Ceylon and Burma, including the whole of the Indo-Chinese Sub-Region. Reptilia and Amphibia (Vol. III). Serpentes. Secretary of State for India, London, xii + 583 pp.

Steindachner F (1891) Über einige neue und seltene Reptilien- und Amphibienarten. Sitzungsberichte der Mathematisch-Naturwissenschaftliche Classe der Kaiserlichen Akademie der Wissenschaften 100: 289–313. [+ Taf. 1–2.]

Steindachner F (1914) Bericht über die von Hans Sauter auf Formosa gesammelten Schlangenarten. Denkschriften der Kaiserlichen Akademie der Wissenschaften in Wien 90: 319–361. [+ 4 pls.]

Stephens M, Smith N, Donnelly P (2001) A new statistical method for haplotype reconstruction from population data. American Journal of Human Genetics 68(4): 978–989. https://doi.org/10.1086/319501

Taylor EH (1922) The Snakes of the Philippine Islands. Bureau of Printing, Manila, 312 pp. https://doi.org/10.5962/bhl.title.55346

Tian S, Kou Y, Zhang Z, Yuan L, Li D, López-Pujol J, Fan D, Zhang Z (2018) Phylogeography of *Eomecon chionantha* in subtropical China: The dual roles of the Nanling Mountains as a glacial refugium and a dispersal corridor. BMC Evolutionary Biology 18: 1–20. https://doi.org/10.1186/s12862-017-1093-x

Tillack F, Günther R (2009) Revision of the species of *Oligodon* from Sumatra and adjacent islands, with comments on the taxonomic status of *Oligodon subcarinatus* (Günther, 1872) and *Oligodon annulifer* (Boulenger, 1893) from Borneo (Reptilia, Squamata, Colubridae. Russian Journal of Herpetology 16(4): 265–294.

Van Denburgh J (1909) New and previously unrecorded species of reptiles and amphibians from the island of Formosa. Proceedings of the California Academy of Sciences, series 4 3: 49–56.

Vences M, Miralles A, Brouillet S, Ducasse J, Fedosov A, Kharchev V, Kostadinov I, Kumari S, Patmanidis S, Scherz MD, Puillandre N, Renner SS (2021) iTaxoTools 0.1: Kickstarting a specimen-based software toolkit for taxonomists. Megataxa 6: 77–92. https://doi.org/10.11646/megataxa.6.2.1

Vences M, Patmanidis S, Schmidt JC, Matschiner M, Miralles A, Renner SS (2024) Hapsolutely: A user-friendly tool integrating haplotype phasing, network construction, and haploweb calculation. Bioinformatics Advances 4(1): vbae083. https://doi.org/10.1093/bioadv/vbae083

Wall F (1909) A second specimen of the snake *Oligodon erythrogaster* from eastern Himalayas. Journal of the Bombay Natural History Society 19(4): 1000–1001.

Wall F (1922) A new snake from the northern frontier of Assam. Records of the Indian Museum 24(1): 29–34. https://doi.org/10.26515/rzsi/v24/i1/1922/163468

Wall F (1923) A review of the Indian species of the genus *Oligodon* suppressing the genus *Simotes* (Ophidia). Records of the Indian Museum 25(3): 305–334. https://doi.org/10.26515/rzsi/v25/i3/1923/162698

Whitaker R, Dattatri S (1982) A new species of *Oligodon* from the Palni Hills, south India (Serpentes: Colubridae). Journal of the Bombay Natural History Society 79(3): 630–631.

Wu L, Li DJ, Xu RH, Dong Q, Liu JS (1979) New species and new records of reptiles from Guizhou Provinces. Academiae Medicinae Zunyi 1979: 104–110. [in Chinese]

Wu L, Li D-J, Liu J-S (1985) Reptile fauna of Guizhou. Guizhou Peoples Press, Guiyang, iv + 436 pp. [67 pls.] [in Chinese]

Wu YH, Hou SB, Yuan ZY, Jiang K, Huang RY, Wang K, Liu Q, Yu ZB, Zhao HP, Zhang BL, Chen JM, Wang LJ, Stuart BL, Chambers EA, Wang YF, Gao W, Zou DH, Yan F, Zhao GG, Fu ZX, Wang SN, Jiang M, Zhang L, Ren JL, Wu YY, Zhang LY, Yang DC, Jin JQ, Yin TT, Li JT, Zhao WG, Murphy RW, Huang S, Guo P, Zhang YP, Che J (2023) DNA barcoding of Chinese snakes reveals hidden diversity and conservation needs. Molecular Ecology Resources 23(5): 1124–1141. https://doi.org/10.1111/1755-0998.13784

Yu G-H, Du L-N, Wang J-S, Rao D-Q, Wu Z-J, Yang J-X (2020) From mainland to islands: colonization history in the tree frog *Kurixalus* (Anura: Rhacophoridae). Current Zoology 66(6): 667–675. https://doi.org/10.1093/cz/zoaa023

Yuan ZY, Jiang K, Rao DQ, Zhang J (2010) A new record of snakes in Hunan Province, *Oligodon lungshenensis*. Sichuan Journal of Zoology 29(3): e367. [in Chinese]

Yushchenko PV, Lee JL, Pham HM, Geissler P, Syromyatnikova EV, Poyarkov NA (2023a) The taxonomic status of the kukri snake *Oligodon arenarius* Vassilieva, 2015 with a redescription of *Oligodon macrurus* (Angel, 1927) (Squamata, Serpentes, Colubridae). Vertebrate Zoology 73: 97–125. https://doi.org/10.3897/vz.73.e96958

Yushchenko PV, Lee JL, Neang T, Seiha H, Tan NV, Vogel G, Poyarkov NA (2023b) A taxonomic re-assessment of *Oligodon cinereus* (Günther, 1864) (Squamata, Serpentes, Colubridae) populations from southern Indochina. Vertebrate Zoology 73: 75–96. https://doi.org/10.3897/vz.73.e91230

Zhang FJ, Hu SQ, Zhao EM (1984) Comparative studies and phylogenetic discussions on hemipenial morphology of the Chinese Colubrinae (Colubridae). Acta Herpetologica Sinica 3(3): 23–44. [in Chinese]

Zhao E (1990) Herpetofauna and zoogeography of Hainan Island. In: Zhao E (Ed.) From water onto land: A volume issued to commemorate the ninetieth birthday of the late professor Liu Cheng-Zhao. China Forestry Publishing House, Beijing, 354–363.

Zhao EM (2002) Coloured atlas of Sichuan reptiles. China Forestry Publishing House, Chengdu, vii + 292 pp. [in Chinese]

Zhao EM (2006) Snakes of China (Vols. 1–2). Anhui Science and Technology Publishing House, Hefei, 372 pp. [+ 279 pp.] [in Chinese]

Zhao EM, Adler K (1993) Herpetology of China. Contributions to Herpetology, No. 10. Society for the Study of Amphibians and Reptiles, Oxford, 522 pp. [+ 48 pls.]

Zhao EM, Yang DT [Eds] (1997) Amphibians and reptiles of the Hengduan Mountains region. Science Press, Beijing, 2 + xiv + 303 pp. [+ 8 pls.] [in Chinese]

Zhao EM, Liu XB, Kang SH (1986) Five snake species new to Sichuan. Acta Herpetologica Sinica 5(2): e157. [in Chinese]

Zhao EM, Huang MH, Zong Y, Zheng J, Huang ZJ, Yang D, Li DJ [Eds] (1998) Fauna Sinica. Reptilia (Vol. 3). Squamata Serpentes. Science Press, Beijing, xvii + 522 pp. [+ 8 pls. + 4 color pls.] [in Chinese]

Zhao HT, Wang LY, Yuan JY (2007) Origin and time of Qiongzhou Strait. Haiyang Dizhi Yu Disiji Dizhi 27(2): 33–40.

Zhou Z, Jiang J, Lau M (2012) *Oligodon lungshenensis*. The IUCN Red List of Threatened Species 2012: e.T191941A2018656. https://doi.org/10.2305/IUCN.UK.2012-1.RLTS.T191941A2018656.en[Accessed on 11 January 2026]

Zhu H (2016) Biogeographical evidences help revealing the origin of Hainan Island. PLoS ONE 11: e0151941. https://doi.org/10.1371/journal.pone.0151941

Zhu H (2025) New insight into the origin and evolution of the flora and fauna of Hainan Island, China. Science China. Earth Sciences 68: 52–61. https://doi.org/10.1007/s11430-024-1440-3

Zhu F, Liu Q, Che J, Zhang L, Chen X, Yan F, Murphy R, Guo C, Guo P (2016) Molecular phylogeography of white-lipped tree viper (*Trimeresurus*, Viperidae). Zoologica Scripta 45(3): 252–262. https://doi.org/10.1111/zsc.12156

Supplementary material 1

Supplementary figures and tables

Authors: Yuhao Xu, Tierui Zhang, Benjamin W. Genter, Bo Cai, Shuo Qi, Shun Ma, Fanyue Sun, Chenxi Liao, Nikolay A. Poyarkov, Gernot Vogel, Justin L. Lee, Lifang Peng

Data type: zip

Explanation note: **table S1.** Verified localities or populations of *O. bivirgatus*, *O. lungshenensis*, and *O. ornatus* used to generate the map in Fig. 1. These localities are based on vouchered material, literature records, and electronic records (i.e., iNaturalist, https://www.inaturalist.org/home; last accessed 1 December 2025). **table S2.** List of primers used in this study to generate DNA sequences. **table S3.** List of genetic samples, accompanying voucher numbers, locality details, and GenBank accession numbers for all *Oligodon* species used in this study. "/" indicates not available. **table S4.** Morphological dataset of *O. bivirgatus*, *O. lungshenensis*, and *O. ornatus* based on examined material and specimens with associated literature data. Refer to the Materials and methods for abbreviations of morphological characters. "/" indicates not available. **table S5.** Morphological dataset of *O. bivirgatus*, *O. lungshenensis*, and *O. ornatus* pruned to characters used for statistical analyses (ANOVA, Tukey's HSD post hoc tests, and PCA). Refer to the Materials and methods for abbreviations of morphological character. **table S6.** Summary statistics from the principal components analysis (PCA) comparing morphological traits of *O. bivirgatus*, *O. lungshenensis*, and *O. ornatus*. Refer to the Materials and methods for morphological character acronyms. **fig. S1.** Phylogenetic relationships of the *O. ornatus* group based on an ML tree of *COI* barcode sequences only. **fig. S2.** Preserved specimen of the holotype of *Simotes musyi* (NHMB unnumbered, adult male, from Wuyishan, Fujian, China). Photographs by G. Vogel.

Copyright notice: This dataset is made available under the Open Database License (http://opendatacommons.org/licenses/odbl/1.0/). The Open Database License (ODbL) is a license agreement intended to allow users to freely share, modify, and use this Dataset while maintaining this same freedom for others, provided that the original source and author(s) are credited.

Link: https://doi.org/10.3897/zse.102.183157.suppl1